



CMS-FSQ-16-004

 CERN-EP-2017-091
2017/12/16

Measurement of charged pion, kaon, and proton production in proton-proton collisions at $\sqrt{s} = 13 \text{ TeV}$

The CMS Collaboration^{*}

Abstract

Transverse momentum spectra of charged pions, kaons, and protons are measured in proton-proton collisions at $\sqrt{s} = 13 \text{ TeV}$ with the CMS detector at the LHC. The particles, identified via their energy loss in the silicon tracker, are measured in the transverse momentum range of $p_T \approx 0.1\text{--}1.7 \text{ GeV}/c$ and rapidities $|y| < 1$. The p_T spectra and integrated yields are compared to previous results at smaller \sqrt{s} and to predictions of Monte Carlo event generators. The average p_T increases with particle mass and charged particle multiplicity of the event. Comparisons with previous CMS results at $\sqrt{s} = 0.9, 2.76$, and 7 TeV show that the average p_T and the ratios of hadron yields feature very similar dependences on the particle multiplicity in the event, independently of the center-of-mass energy of the pp collision.

Published in Physical Review D as doi:10.1103/PhysRevD.96.112003.

1 Introduction

The study of hadron production has a long history in high-energy particle, nuclear, and cosmic ray physics. The absolute yields and the transverse momentum (p_T) spectra of identified hadrons in high-energy hadron-hadron collisions are among the most basic physical observables. They can be used to improve the modeling of various key ingredients of Monte Carlo (MC) hadronic event generators, such as multiparton interactions, parton hadronization, and final-state effects (such as parton correlations in color, p_T , spin, baryon and strangeness number, and collective flow) [1]. The dependence of the hadron spectra and yields on the impact parameter of the proton-proton (pp) collision provides additional valuable information to tune the corresponding MC parameters. Indeed, parton hadronization and final-state effects are mostly constrained from elementary e^+e^- collisions, whose final states are largely dominated by simple $q\bar{q}$ final states, whereas low- p_T hadrons at the LHC issue from the fragmentation of multiple gluon “minijets” [1]. Such large differences have a particularly important impact on baryons and strange hadrons, whose production in pp collisions is not well reproduced by the existing models [2, 3], and also affect the modeling of hadronic interactions of ultrahigh-energy cosmic rays with Earth’s atmosphere [4]. Spectra of identified particles in pp collisions also constitute an important reference for high-energy heavy ion studies, where various final-state effects are known to modify the spectral shape and yields of different hadron species [5–9].

The present analysis uses pp collisions collected by the CMS experiment at the CERN LHC at $\sqrt{s} = 13$ TeV and focuses on the measurement of the p_T spectra of charged hadrons, identified primarily via their energy depositions in the silicon detectors. The analysis adopts the same methods as used in previous CMS measurements of pion, kaon, and proton production in pp and pPb collisions at \sqrt{s} of 0.9, 2.76, and 7 TeV [2, 10], as well as those performed by the ALICE Collaboration at 2.76 and 7 TeV [3, 11].

2 The CMS detector and event generators

A detailed description of the CMS detector can be found in Ref. [12]. The CMS experiment uses a right-handed coordinate system, with the origin at the nominal interaction point (IP) and the z axis along the counterclockwise-beam direction. The pseudorapidity η and rapidity y of a particle (in the laboratory frame) with energy E , momentum p , and momentum along the z axis p_z are defined as $\eta = -\ln[\tan(\theta/2)]$, where θ is the polar angle with respect to the z axis and $y = \frac{1}{2}\ln[(E + p_z)/(E - p_z)]$. The central feature of the CMS apparatus is a superconducting solenoid of 6 m internal diameter. Within the 3.8 T field volume are the silicon pixel and strip tracker, the crystal electromagnetic calorimeter, and a brass and scintillator hadron calorimeter. The tracker measures charged particles within the range $|\eta| < 2.4$. It has 1440 silicon pixel and 15 148 silicon strip detector modules with thicknesses of either 300 or 500 μm , assembled in 13 detection layers in the central region. Beam pick-up timing for the experiment (BPTX) devices were used to trigger the detector readout. They are located around the beam pipe at a distance of 175 m from the IP on either side, and are designed to provide precise information on the bunch structure and timing of the incoming beams of the LHC.

In this paper, distributions of identified hadrons produced in inelastic pp collisions are compared to predictions from MC event generators based on two different theoretical frameworks: perturbative QCD (PYTHIA6.426 [13] and PYTHIA8.208 [14]) and Reggeon field theory (EPOS v3400 [15]). On the one hand, the basic ingredients of PYTHIA6 and PYTHIA8 are (multiple) leading-order perturbative QCD $2 \rightarrow 2$ matrix elements, complemented with initial- and final-state parton radiation (ISR and FSR), folded with parton distribution functions in the proton, and the Lund

string model for parton hadronization. Two different “tunes” of the parameters governing the nonperturbative and semihard dynamics (ISR and FSR showering, multiple parton interactions, beam-remnants, final-state color-reconnection, and hadronization) are used: the PYTHIA6 Z2* [13, 16] and PYTHIA8 CUETP8M1 [16] tunings, based on fits to recent minimum bias and underlying event measurements at the LHC. On the other hand, EPOS starts off from the basic quantum field-theory principles of unitarity and analyticity of scattering amplitudes as implemented in Gribov’s Reggeon field theory [17], extended to include (multiple) parton scatterings via “cut (hard) Pomerons.” The latter objects correspond to color flux tubes that are finally hadronized also via the Lund string model. The version of EPOS used here is run with the LHC tune [18] which includes collective final-state string interactions resulting in an extra radial flow of the final hadrons produced in more central pp collisions.

3 Event selection and reconstruction

The data used for the measurements presented in this paper were taken during a special low luminosity run where the average number of pp interactions in each bunch crossing was 1.0. A total of 7.0×10^6 collisions were recorded, corresponding to an integrated luminosity of approximately 0.1 nb^{-1} .

The event selection consisted of the following requirements:

- at trigger level, the coincidence of signals from both BPTX devices, indicating the presence of both proton bunches crossing the interaction point;
- offline, to have at least one reconstructed interaction vertex;
- beam-halo and beam-induced background events, which usually produce an anomalously large number of pixel hits, were identified [19] and rejected.

The event selection efficiency as well as the tracking and vertexing acceptance and efficiency are evaluated using simulated event samples produced with the PYTHIA8 (tune CUETP8M1) MC event generator, followed by the CMS detector response simulation based on GEANT4 [20]. Simulated events are reconstructed and analyzed in the same way as collision data events. The final results are given for an event selection corresponding to inelastic pp collisions, which will be presented in Sec. 6. According to the three MC event generators considered, the fraction of inelastic pp collisions not resulting in a reconstructed pp interaction amounts to about $14\% \pm 3\%$, where the uncertainty is based on the variance of the predictions coming from the event generators. These events are mostly diffractive ones with negligible central activity.

The reconstruction of charged particles in CMS is limited by the acceptance of the tracker ($|\eta| < 2.4$) and by the decreasing tracking efficiency at low momentum caused by multiple scattering and energy loss. The identification of particle species using specific ionization (Sec. 4) is restricted to $p < 0.15 \text{ GeV}/c$ for electrons, $p < 1.20 \text{ GeV}/c$ for pions, $p < 1.05 \text{ GeV}/c$ for kaons, and $p < 1.70 \text{ GeV}/c$ for protons [2, 10]. Pions are measured up to a higher momentum than kaons because of their larger relative abundance. In order to have a common kinematic region where pions, kaons, and protons can all be identified, the range $|y| < 1$ is chosen for this measurement.

The extrapolation of particle spectra into unmeasured (y, p_T) regions is model dependent, particularly at low p_T . A precise measurement therefore requires reliable track reconstruction down to the lowest possible p_T values. Special tracking algorithms [21], already used in previous studies [2, 10, 19, 22], made it possible to extend the present analysis to $p_T \approx 0.1 \text{ GeV}/c$ with high reconstruction efficiency and low background. Compared to the standard tracking

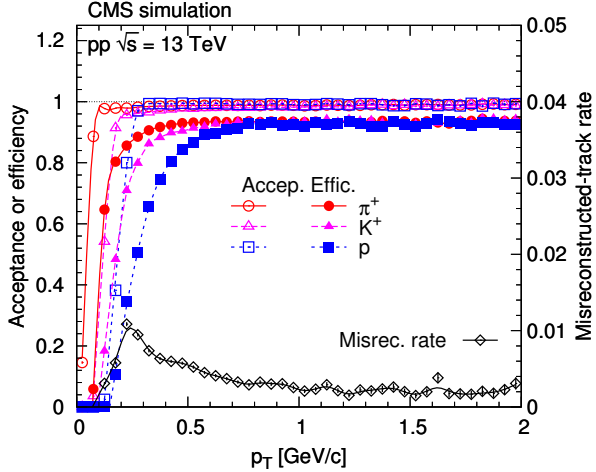


Figure 1: Acceptance (open markers, left scale), tracking efficiency (filled markers, left scale), and misreconstructed-track rate (right scale) in the range $|\eta| < 2.4$ as a function of p_T for positively charged pions, kaons, and protons. The values are very similar for negatively charged particles.

algorithm used in CMS, these algorithms feature special track seeding and cleaning, hit cluster shape filtering, modified trajectory propagation, and track quality requirements. The charged-pion mass is assumed when fitting particle momenta.

The acceptance of the tracker (C_a) is defined as the fraction of primary charged particles leaving at least two hits in the pixel detector. Based on MC studies, it is flat in the region $|\eta| < 2$ and $p_T > 0.4 \text{ GeV}/c$, and at values of 96%–98% as can be seen in Fig. 1. The loss of acceptance at $p_T < 0.4 \text{ GeV}/c$ is caused by energy loss and multiple scattering, which are both functions of particle mass. The reconstruction efficiency (C_e), which is defined as the fraction of accepted charged particles that result in a successfully reconstructed trajectory, is usually in the range 80%–90%. It decreases at low p_T , also in a mass-dependent way. The misreconstructed-track rate (C_f), defined as the fraction of reconstructed primary charged tracks without a corresponding genuine primary charged particle, is very small, reaching 1% for $p_T < 0.2 \text{ GeV}/c$. The probability of reconstructing multiple tracks (C_m) from a single charged particle is about 0.1%, mostly from particles spiralling in the strong magnetic field of the CMS solenoid. The efficiencies and background rates (misreconstruction, multiple reconstruction) are found not to depend on the charged-particle multiplicity of the event in the range of multiplicities of interest for this analysis. They largely factorize in η and p_T , but for the final corrections (Sec. 5) an (η, p_T) matrix is used.

The region where pp collisions occur (beam spot) is measured from the distribution of reconstructed interaction vertices. Since the bunches are very narrow in the plane transverse to the beam direction (with a width of about $50 \mu\text{m}$ for this special run), the x - y location of the interaction vertices is well constrained; conversely, their z coordinates are spread over a relatively long distance and must be determined on an event-by-event basis. The vertex position is determined using reconstructed tracks that have $p_T > 0.1 \text{ GeV}/c$ and originate from the vicinity of the beam spot, i.e. their transverse impact parameters d_T (with respect to the center of the beam spot) satisfy the condition $d_T < 3\sigma_T$. Here σ_T is the quadratic sum of the uncertainty in the value of d_T and the root mean square of the beam spot distribution in the transverse plane. In order to reach higher efficiency in special-topology low-multiplicity events, an agglomerative vertex reconstruction algorithm [23] is used, with the z coordinates of the tracks (and their uncertainties) at the point of closest approach to the beam axis as input. The distance

distributions of reconstructed vertex pairs in data indicates that the fraction of merged vertices (with tracks from two or more true vertices) and split vertices (two or more reconstructed vertices with tracks from a single true vertex) is about 1%. For single-vertex events, there is no minimum requirement on the number of tracks associated with the vertex (those assigned to it during vertex finding), and even one-track vertices, which are defined as the point of closest approach of the track to the beam line, are allowed. The fraction of events with more than one (three) reconstructed primary vertices is about 26% (1.8%). Only events with three or fewer reconstructed primary vertices were considered and only tracks associated with a primary vertex are used in the analysis.

The vertex resolution in the z direction is a strong function of the number of reconstructed tracks and is always less than 0.1 cm. The distribution of the z coordinates of the reconstructed primary vertices is Gaussian with a width of $\sigma = 4.2$ cm. Simulated events are reweighted in order to have the same vertex z coordinate distribution as in collision data.

The contribution to the hadron spectra from particles of nonprimary origin arising from the decay of particles with proper lifetime $\tau > 10^{-12}$ s was subtracted. The main sources of these secondary particles are weakly decaying particles, mostly K_S^0 , $\Lambda/\bar{\Lambda}$, and $\Sigma^+/\bar{\Sigma}^-$. According to the simulations, this correction (C_s) is approximately 1% for pions and rises to 15% for protons with $p_T \approx 0.2$ GeV/ c . Because none of these particles decay weakly into kaons, the correction for kaons is less than 0.1%. Charged particles from interactions of primary particles or their decay products with detector material are suppressed by the impact parameter cuts described above.

For $p < 0.15$ GeV/ c , electrons can be clearly identified based on their energy loss (Fig. 2, left) and their contamination of the hadron yields is below 0.2%. Although muons cannot be distinguished from pions, according to MC predictions their fraction is below 0.05%. Since both contaminations are negligible with respect to the final uncertainties, no corrections are applied.

4 Estimation of energy loss rate and yield extraction

For this paper an analytical parametrization [24] is used to model the energy loss of charged particles in the silicon detectors. It provides the probability density $P(\Delta|\varepsilon, l)$ of finding an energy deposit Δ , if the most probable energy loss rate ε at a reference path length $l_0 = 450$ μm and the path length l are known. The choice of 450 μm is motivated by being the approximate average path length traversed in the silicon detectors. The value of ε depends on the momentum and mass m of the charged particle. The parametrization is used in conjunction with a maximum likelihood fit for the estimate of ε . All details of the methods described below are given in Ref. [2].

Using the cluster shape filtering mentioned in Sec. 3, only hit clusters compatible with the particle trajectory are used. For clusters in the pixel detector, the energy deposits are calculated based on the individual pixel deposits. In the case of clusters in the strip detector, the energy deposits are corrected for truncation performed by the readout electronics and for losses due to deposits below threshold because of capacitive coupling and cross-talk between neighboring strips. The readout threshold, the strength of coupling, and the standard deviation of the Gaussian noise for strips are determined from data. The response of all readout chips is calibrated with multiplicative gain correction factors.

After the readout chip calibration, the measured energy deposit spectra for each silicon sub-detector are compared to the expectations of the energy loss model as a function of p/m and

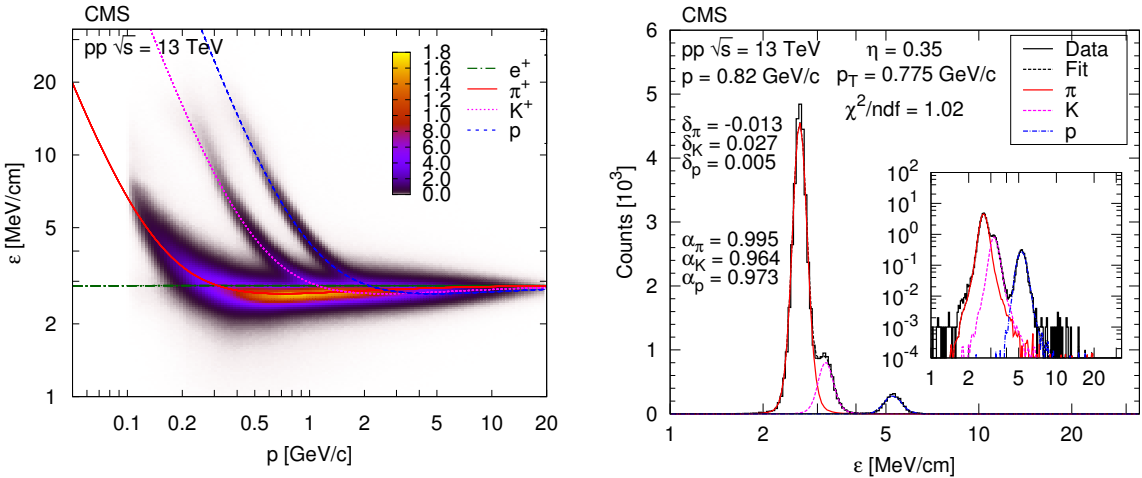


Figure 2: Left: distribution of ϵ as a function of total momentum p , for positively charged reconstructed particles (ϵ is the most probable energy loss rate at a reference path length $l_0 = 450 \mu\text{m}$). The color scale is shown in arbitrary units and is linear. The curves show the expected ϵ for electrons, pions, kaons, and protons (Eq. (30.11) in Ref. [25]). Right: example ϵ distribution at $\eta = 0.35$ and $p_T = 0.775 \text{ GeV}/c$ (bin centers), with bin widths $\Delta\eta = 0.1$ and $\Delta p_T = 0.05 \text{ GeV}/c$. Scale factors (α) and shifts (δ) are indicated. The inset shows the distribution with logarithmic vertical scale.

l using particles satisfying tight identification criteria. These comparisons allow the computation of hit-level corrections to the energy loss model that is used to estimate the particle energy loss rate ϵ and its associated distribution.

The best value of ϵ for each track is calculated from the measured energy deposits by minimizing the negative log-likelihood function of the combined energy deposit for all hits (index i) associated with the particle trajectory, $\chi^2 = -2 \sum_i \ln P(\Delta_i | \epsilon, l_i)$, where the probability density functions include the hit-level corrections mentioned above. Hits with incompatible energy deposits (contributing more than 12 units to the combined χ^2) are excluded. For the determination of ϵ , removal of at most one hit per track is allowed; this affected about 1.5% of the tracks.

Low-momentum particles can be identified unambiguously and can therefore be counted (Fig. 2). Conversely, at high momenta (above about $0.5 \text{ GeV}/c$ for pions and kaons and above $1.2 \text{ GeV}/c$ for protons) the ϵ bands overlap. Therefore the particle yields need to be determined by means of a series of template fits in ϵ , in bins of η and p_T (Fig. 2, right panel). Fit templates with the expected ϵ distributions for all particle species (electrons, pions, kaons, and protons) are obtained from reconstructed tracks in data. All track parameters and hit-related quantities are kept but, in order to populate the distributions, the energy deposits are regenerated by sampling from the hit-level corrected analytical parametrization assuming a given particle type. Possible residual discrepancies between the observed and expected ϵ distributions, present in some regions of the parameter space (mostly at low p_T), are taken into account by means of the track-level corrections consisting, as for the hit-level corrections, of a linear transformation of the parametrization using scale factors and shifts. For a less biased determination of these track-level residual corrections, enriched samples of each particle type are employed for determining starting values of the parameters to be fitted. For electrons and positrons, photon conversions in the beam-pipe and in the innermost pixel layer are used. For high-purity pion and enriched proton samples, weakly decaying hadrons are selected ($K_S^0, \Lambda/\bar{\Lambda}$). The following criteria and methods described in Ref. [2] are also exploited to better constrain the parameters of the fits:

fitting the ε distributions in slices of number of hits (n_{hits}) and track fit χ^2/ndf (where ndf is number of degrees of freedom) simultaneously; setting constraints on the n_{hits} distribution for specific particle species; imposing the expected continuity of track-level residual corrections in adjacent (η, p_{T}) bins; and using the expected convergence of track-level residual corrections as the ε values of two particle species approach each other at large momentum.

Distributions of ε as a function of total momentum p for positive particles are plotted in the left panel of Fig. 2 and compared to the predictions of the energy loss parametrization [24] for electrons, pions, kaons, and protons. The results of the (iterative) ε fits are the yields for each particle species and charge in bins of (η, p_{T}) or (y, p_{T}) , both inclusive and divided into classes of reconstructed primary charged-track multiplicity. Although pion and kaon yields could not be determined for $p > 1.30 \text{ GeV}/c$, their sum is measured. This information is an important constraint when fitting the p_{T} spectra.

5 Yield extraction and systematic uncertainties

The measured yields in each (η, p_{T}) bin, $\Delta N_{\text{measured}}$, are first corrected for the misreconstructed-track rate C_f and the fraction of secondary particles C_s :

$$\Delta N' = \Delta N_{\text{measured}} (1 - C_f) (1 - C_s). \quad (1)$$

The bin widths are $\Delta\eta = 0.1$ and $\Delta p_{\text{T}} = 0.05 \text{ GeV}/c$. The distributions are then unfolded to take into account bin migrations due to the finite η and p_{T} resolutions. The η distribution of the tracks is almost flat and the η resolution is significantly smaller than the bin width. At the same time the p_{T} distribution is steep in the low-momentum region and separate p_{T} -dependent corrections in each η slice are necessary. For that, an unfolding procedure with a linear regularization method (Tikhonov regularization [26]) is used, based on response matrices obtained from PYTHIA8 MC samples separately for each particle species. This procedure guarantees that the uncertainties associated with the assumption of the pion mass in the track fitting step are taken into account. The bin purities of the matrices are above 80%–90%. The chosen regularization term reflects that the original distribution changes only slowly, but that that particular choice has negligible influence on the results.

Further corrections for acceptance, efficiency, and multiple track reconstruction probability are applied:

$$\frac{1}{N_{\text{ev}}} \frac{d^2N}{d\eta dp_{\text{T}}}_{\text{corrected}} = \frac{1}{C_a C_e (1 + C_m)} \frac{\Delta N'}{N_{\text{ev}} \Delta\eta \Delta p_{\text{T}}}, \quad (2)$$

where N_{ev} is the corrected number of inelastic pp collisions in the data sample. Bins that meet at least one of the following criteria are not used in order to ensure robustness of the fits described below and to minimize the impact on the systematic uncertainties: acceptance less than 50%; efficiency less than 50%; multiple-track rate greater than 10%; multiplicity below 80 tracks.

Finally, the η -differential yields $d^2N/d\eta dp_{\text{T}}$ are transformed into $d^2N/dy dp_{\text{T}}$ yields by multiplying with the Jacobian of the η to y transformation (E/p), and the (η, p_{T}) bins are mapped onto a (y, p_{T}) grid. The differential yields exhibit a slight (5%–10%) dependence on y in the narrow region considered ($|y| < 1$), an effect that decreases with the event multiplicity. The yields as a function of p_{T} are obtained averaged over the rapidity window.

The p_T distributions are fit using a Tsallis-Pareto-type function, which empirically describes both the low- p_T exponential and the high- p_T power-law behaviors while employing only a few parameters. Based on the good reproduction of previous measurements of unidentified and identified particle spectra [2, 10, 19, 27], the following form of the distribution [28, 29] is used:

$$\frac{d^2N}{dy dp_T} = \frac{dN}{dy} C p_T \left[1 + \frac{m_T - m c}{nT} \right]^{-n}, \quad (3)$$

where

$$C = \frac{(n-1)(n-2)}{nT[nT + (n-2)m c]} \quad (4)$$

and $m_T = \sqrt{(mc)^2 + p_T^2}$. The free parameters are the integrated yield dN/dy , the exponent n , and the parameter T . According to some models of particle production based on nonextensive thermodynamics [29], the parameter T is connected with the average particle energy, while n characterizes the “nonextensivity” of the process, i.e. the departure of the spectra from a Boltzmann distribution ($n = \infty$). Equation (3) is useful for extrapolating the spectra down to zero and up to high p_T , and thereby extracting $\langle p_T \rangle$ and $\langle dN/dy \rangle$. Its validity for different multiplicity bins is cross-checked by fitting MC spectra in the p_T ranges where there are data points, and verifying that the fitted values of $\langle p_T \rangle$ and $\langle dN/dy \rangle$ are consistent with the generated values. Nevertheless, for a more robust estimation of both $\langle p_T \rangle$ and $\langle dN/dy \rangle$, the unfolded bin-by-bin yield values and their uncertainties are used in the measured range while the fitted functions are employed for the extrapolation into the unmeasured regions.

As discussed earlier, pions and kaons cannot be unambiguously distinguished at high momenta. For this reason the pion-only, the kaon-only, and the joint pion and kaon $d^2N/dy dp_T$ distributions are fitted for $|y| < 1$ and $p < 1.20 \text{ GeV}/c$, $|y| < 1$ and $p < 1.05 \text{ GeV}/c$, and $|\eta| < 1$ and $1.05 < p < 1.7 \text{ GeV}/c$, respectively. Since the ratio p/E for the pions (which are more abundant than kaons) at these momenta can be approximated by p_T/m_T at $\eta \approx 0$, Eq. (3) becomes:

$$\frac{d^2N}{d\eta dp_T} \approx \frac{dN}{dy} C \frac{p_T^2}{m_T} \left(1 + \frac{m_T - m c}{nT} \right)^{-n}. \quad (5)$$

Moreover, below p_T values of 0.1–0.3 GeV the detector acceptance and the tracking efficiency significantly decrease. The Tsallis-Pareto function is used to extrapolate the measured yields both into this latter region and to the region at high momenta such that the integrated yield (dN/dy) and the average transverse momentum ($\langle p_T \rangle$) can be reported for the full p_T range. This choice allows measurements performed by different experiments in various collision systems and center-of-mass energies to be compared.

The fractions of particles outside the measured p_T range are 15%–30% for pions, 40%–50% for kaons, and 20%–35% for protons, depending on the track multiplicity of the event.

The systematic uncertainties are very similar to those in Ref. [2] and are summarized in Table 1. They are obtained from the comparison of different MC event generators, differences between data and simulation, or based on previous studies (hit inefficiency, misalignment). The uncertainties in the corrections C_a , C_e , C_f and C_m , which are related to the event selection, and the effects of pileup, are fully or mostly correlated and are treated as normalization uncertainties:

altogether they propagate to a 3.0% uncertainty in the yields and a 1.0% uncertainty in the average p_T . In order to study the influence of the high- p_T extrapolation on the $\langle dN/dy \rangle$ and $\langle p_T \rangle$ averages, the reciprocal of the exponent ($1/n$) of the fitted Tsallis-Pareto function was increased and decreased by ± 0.05 only in the region above the highest measured p_T ; in this same region both the function and its first derivative were required to fit continuously the data points. The choice of the magnitude for the variation is motivated by the fitted $1/n$ values and their distance from a Boltzmann distribution. The resulting functions are plotted in Fig. 3 as dotted lines (though they are mostly indistinguishable from the nominal fit curves). The high- p_T extrapolation introduces systematic uncertainties of 1–3% for $\langle dN/dy \rangle$, and 4–8% for $\langle p_T \rangle$. The systematic uncertainty related to the low p_T extrapolation is small compared to the contributions from other sources and therefore is not included in the combined systematic uncertainty of the measurement.

The tracker acceptance and the track reconstruction efficiency generally have small uncertainties (1 and 3%, respectively), but at very low p_T they reach 6%. For the multiple-track and misreconstructed-track rate corrections, the uncertainty is assumed to be 50% of the correction, while for the correction for secondary particles it is estimated to be 25% based on the differences between predictions of MC event generators and data. These bin-by-bin, largely uncorrelated uncertainties are caused by the imperfect modeling of the detector: regions with incorrectly modeled tracking efficiency, alignment uncertainties, and channel-by-channel varying hit efficiency. All these effects are taken as uncorrelated.

The statistical uncertainties in the extracted yields are given by the fit uncertainties. Variations of the track-level correction parameters, incompatible with statistical fluctuations, are observed. They are used to estimate the systematic uncertainties in the fitted scale factors and shifts and are at the level of 10^{-2} and 2×10^{-3} , respectively. The systematic uncertainties in the yields in each bin are thus obtained by refitting the histograms with the parameters changed by these amounts. For the present measurement, systematic uncertainties dominate over the statistical ones.

The systematic uncertainties originating from the unfolding procedure are also studied. Since the p_T response matrices are close to diagonal, the unfolding of the p_T distributions does not introduce substantial uncertainties. The correlations between neighboring p_T bins are neglected, and therefore statistical uncertainties are regarded as uncorrelated. The systematic uncertainty of the fitted yields is in the range 1%–10%, depending primarily on total momentum.

6 Results

The results discussed in the following are averaged over the rapidity range $|y| < 1$. In all cases, error bars in the figures indicate the uncorrelated statistical uncertainties, while boxes show the uncorrelated systematic uncertainties. The fully correlated normalization uncertainty is not shown. For the p_T spectra, the average transverse momentum $\langle p_T \rangle$, and the ratios of particle yields, the data are compared to the predictions of PYTHIA8, EPOS, and PYTHIA6.

6.1 Inclusive measurements

The transverse momentum distributions of positively and negatively charged hadrons (pions, kaons, protons) are shown in Fig. 3, along with the results of the fits to the Tsallis-Pareto parametrization [Eqs. (3) and (5)]. The fits are of good quality with χ^2/ndf values in the range 0.4–1.2 (Table 2). Figure 4 presents the same data compared to the PYTHIA8, EPOS, and PYTHIA6 predictions. While pions are described well by all three generators, kaons are best modelled by

Table 1: Summary of the systematic uncertainties affecting the p_T spectra. Values in parentheses indicate uncertainties in the $\langle p_T \rangle$ measurement. Representative, particle-specific uncertainties (π , K , p) are given for $p_T = 0.6 \text{ GeV}/c$ in the third group of systematic uncertainties.

Source	Uncertainty of the source [%]	Propagated yield uncertainty [%]		
Fully correlated, normalization	3.0 (1.0) 0.3 1–3 (4–8)		3–4 (5–9)	
Correction for event selection				
Pileup correction (merged and split vertices)				
High- p_T extrapolation				
Mostly uncorrelated	0.3 0.1		0.3	
Pixel hit efficiency				
Misalignment, different scenarios				
Mostly uncorrelated, (y, p_T) -dependent	1–6 3–6 50% of the corr. 50% of the corr. 25% of the corr. 1–10	π 1 3 — 0.1 0.2 1	K 1 3 — 0.1 — 2	p 1 3 — 0.1 — 1
Acceptance of the tracker				
Efficiency of the reconstruction				
Multiple-track reconstruction				
Misreconstructed-track rate				
Correction for secondary particles				
Fit of the ε distributions				

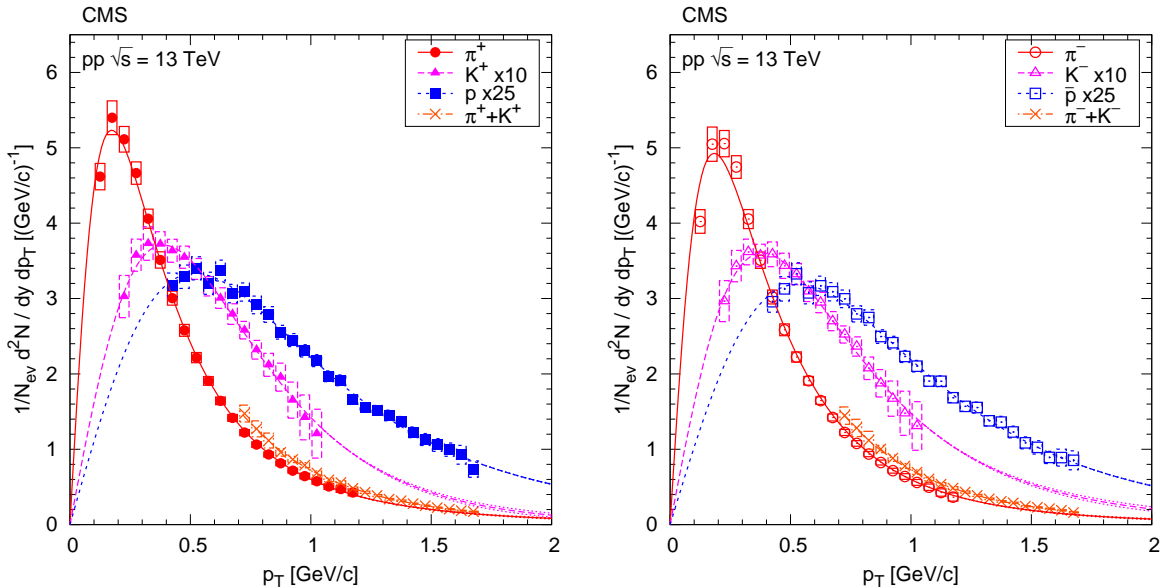


Figure 3: Transverse momentum distributions of identified charged hadrons (pions, kaons, protons, sum of pions and kaons) from inelastic pp collisions, in the range $|y| < 1$, for positively (left) and negatively (right) charged particles. Kaon and proton distributions are scaled as shown in the legends. Fits to Eqs. (3) and (5) are superimposed. For the $\pi+K$ fit, only the region corresponding to the range $|\eta| < 1$ and $1.05 < p < 1.7 \text{ GeV}/c$ is plotted. Boxes show the uncorrelated systematic uncertainties, while error bars indicate the uncorrelated statistical uncertainties (barely visible). The fully correlated normalization uncertainty (not shown) is 3.0%. Dotted lines (mostly indistinguishable from the nominal fit curves) illustrate the effect of varying the inverse exponent ($1/n$) of the Tsallis-Pareto function by ± 0.05 beyond the highest- p_T measured point.

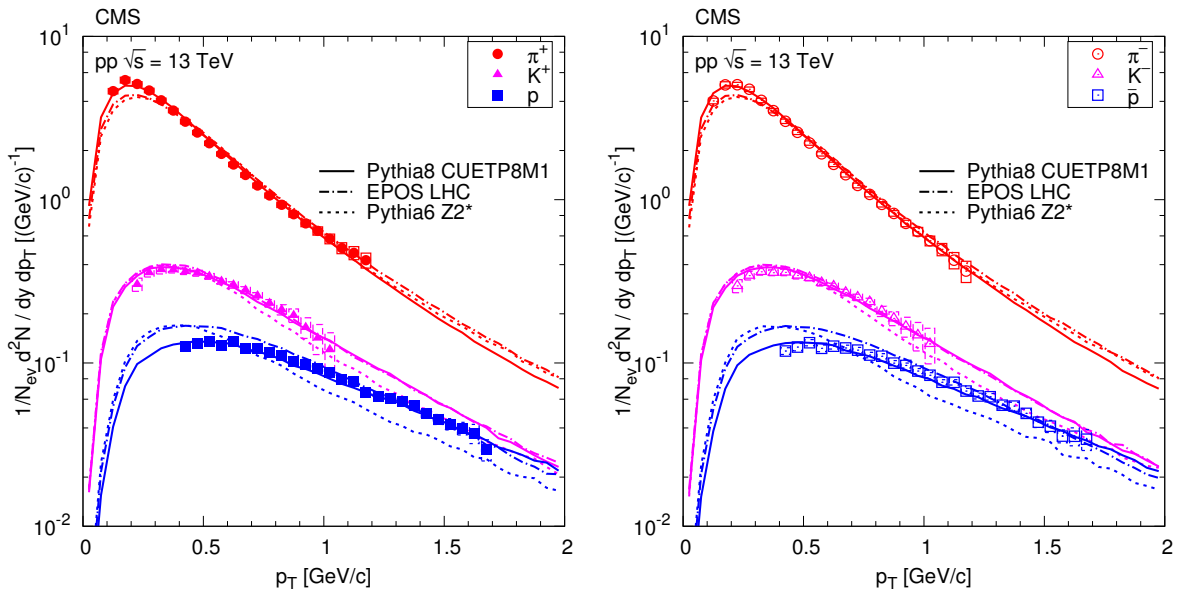


Figure 4: Transverse momentum distributions of identified charged hadrons (pions, kaons, protons) from inelastic pp collisions, in the range $|y| < 1$, for positively (left) and negatively (right) charged particles. Measured values (same as in Fig. 3) are plotted together with predictions from PYTHIA8, EPOS, and PYTHIA6. Boxes show the uncorrelated systematic uncertainties, while error bars indicate the uncorrelated statistical uncertainties (hardly visible). The fully correlated normalization uncertainty (not shown) is 3.0%.

Table 2: Fit results for dN/dy , n , and T (obtained via Eqs. (3) and (5)), associated goodness-of-fit values, and extracted $\langle dN/dy \rangle$ and $\langle p_T \rangle$ averages, for charged pion, kaon, and proton spectra measured in the range $|y| < 1$ in inelastic pp collisions at 13 TeV. Combined statistical and systematic uncertainties are given.

Particle	dN/dy	n	T [GeV/c]	χ^2/ndf	$\langle dN/dy \rangle$	$\langle p_T \rangle$ [GeV/c]
π^+	2.833 ± 0.031	5.2 ± 0.2	0.119 ± 0.003	6.8/19	2.843 ± 0.034	0.51 ± 0.03
π^-	2.733 ± 0.029	5.9 ± 0.2	0.130 ± 0.003	22/19	2.746 ± 0.031	0.50 ± 0.03
K^+	0.318 ± 0.021	15 ± 18	0.231 ± 0.025	7.3/14	0.318 ± 0.007	0.67 ± 0.03
K^-	0.332 ± 0.026	7.7 ± 4.6	0.217 ± 0.024	5.0/14	0.331 ± 0.011	0.75 ± 0.05
p	0.169 ± 0.007	4.7 ± 0.8	0.222 ± 0.016	8.9/23	0.169 ± 0.004	1.10 ± 0.12
\bar{p}	0.162 ± 0.006	5.3 ± 1.1	0.237 ± 0.016	8.4/23	0.162 ± 0.004	1.07 ± 0.09

PYTHIA8 and EPOS. For protons and very low p_T pions only PYTHIA8 gives a good description of the data.

Ratios of particle yields as a function of the transverse momentum are plotted in Fig. 5. Only PYTHIA8 is able to predict both the K/π and p/π ratios as a function of p_T . The ratios of the yields for oppositely charged particles are close to one (Fig. 5, right), as expected at this center-of-mass energy in the central rapidity region.

6.2 Multiplicity-dependent measurements

The study of the p_T spectra as a function of the event track multiplicity is motivated partly by the intriguing hadron correlations measured in pp and pPb collisions at high track multiplicities [30–33], suggesting possible collective effects in “central” collisions at the LHC. We have also observed that in pp collisions at LHC energies [2, 10], the characteristics of particle

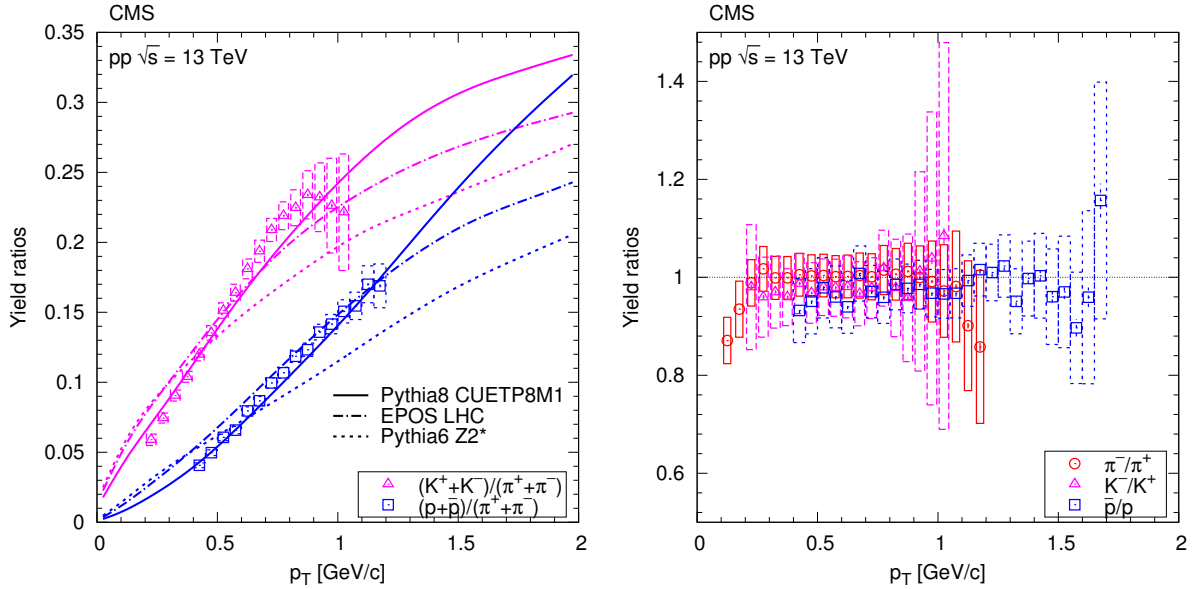


Figure 5: Ratios of particle yields, K/π and p/π (left) and opposite-charge ratios (right), as a function of transverse momentum. Error bars indicate the uncorrelated statistical uncertainties, while boxes show the uncorrelated systematic uncertainties. In the left panel, curves indicate predictions from PYTHIA8, EPOS, and PYTHIA6.

Table 3: Relationship between the number of reconstructed tracks (N_{rec}) and the average number of corrected tracks ($\langle N_{\text{tracks}} \rangle$) in the region $|\eta| < 2.4$ in the 18 multiplicity classes considered.

N_{rec}	0–9	10–19	20–29	30–39	40–49	50–59	60–69	70–79	80–89	90–99	100–109	110–119	120–129	130–139	140–149	150–159	160–169	170–179
$\langle N_{\text{tracks}} \rangle$	7	16	28	40	51	63	74	85	97	108	119	130	141	151	162	172	183	187

production ($\langle p_T \rangle$, ratios of yields) are strongly correlated with the particle multiplicity in the event, which is in itself closely related to the number of underlying parton-parton interactions, independently of the concrete center-of-mass energy of the pp collision.

The event track multiplicity, N_{rec} , is defined as the number of tracks with $|\eta| < 2.4$ reconstructed using the same algorithm as for the identified charged hadrons [21]. The event multiplicity is divided into 18 classes as defined in Table 3. To facilitate comparisons with models, the event charged-particle multiplicity over $|\eta| < 2.4$ (N_{tracks}) is determined for each multiplicity class by correcting N_{rec} for the track reconstruction efficiency, which is estimated with the PYTHIA8 simulation in (η, p_T) bins. The corrected yields are then integrated over p_T , down to zero yield at $p_T = 0$ (with a linear extrapolation below $p_T = 0.1 \text{ GeV}/c$). Finally, the integrals for each η slice are summed up. The average corrected charged-particle multiplicity $\langle N_{\text{tracks}} \rangle$ is shown in Table 3 for each event multiplicity class. The value of $\langle N_{\text{tracks}} \rangle$ is used to identify the multiplicity class in Figs. 6–9.

Transverse-momentum distributions of pions, kaons, and protons, measured over $|\eta| < 1$ and normalized such that the fit integral is unity, are shown in Fig. 6 for various multiplicity classes. The distributions of negatively and positively charged particles are summed. The Tsallis-Pareto parametrization is fitted to the distributions with χ^2/ndf values in the range 0.3–2.3 for pions, 0.2–2.6 for kaons, and 0.1–0.8 for protons. It is observed that for kaons and protons, the parameter T increases with multiplicity, while for pions T slightly increases and the exponent n

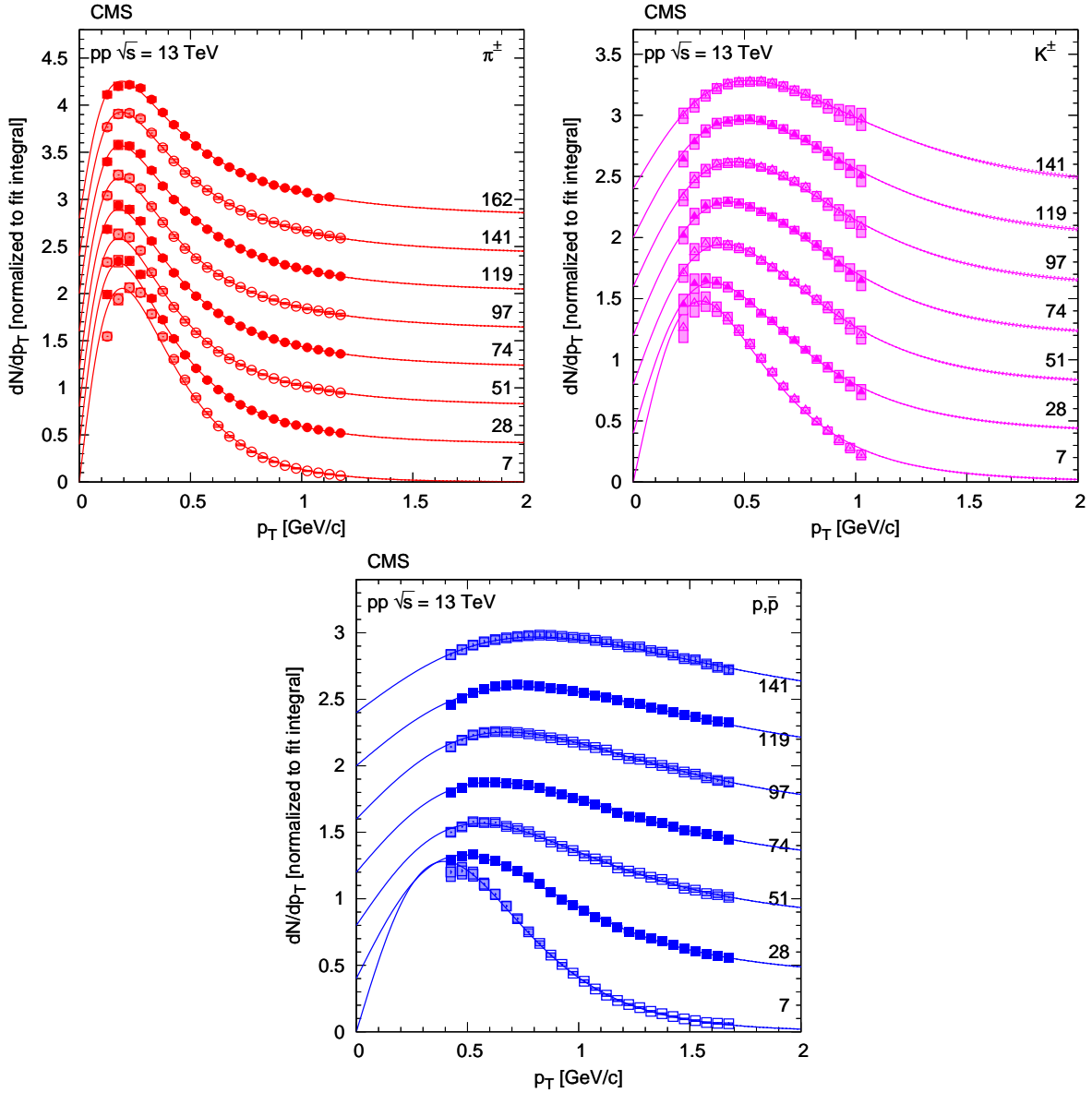


Figure 6: Transverse momentum distributions of charged pions (top left), kaons (top right), and protons (bottom), normalized such that the fit integral is unity, in every selected multiplicity class ($\langle N_{\text{tracks}} \rangle$ values are indicated) in the range $|y| < 1$, fitted with the Tsallis-Pareto parametrization (solid lines). For better visibility, the result for any given $\langle N_{\text{tracks}} \rangle$ bin is shifted by 0.4 units with respect to the adjacent bins. Error bars indicate the uncorrelated statistical uncertainties, while boxes show the uncorrelated systematic uncertainties. Dotted lines (mostly indistinguishable from the nominal fit curves) illustrate the effect of varying the inverse exponent ($1/n$) of the Tsallis-Pareto function by ± 0.05 beyond the highest- p_T measured point.

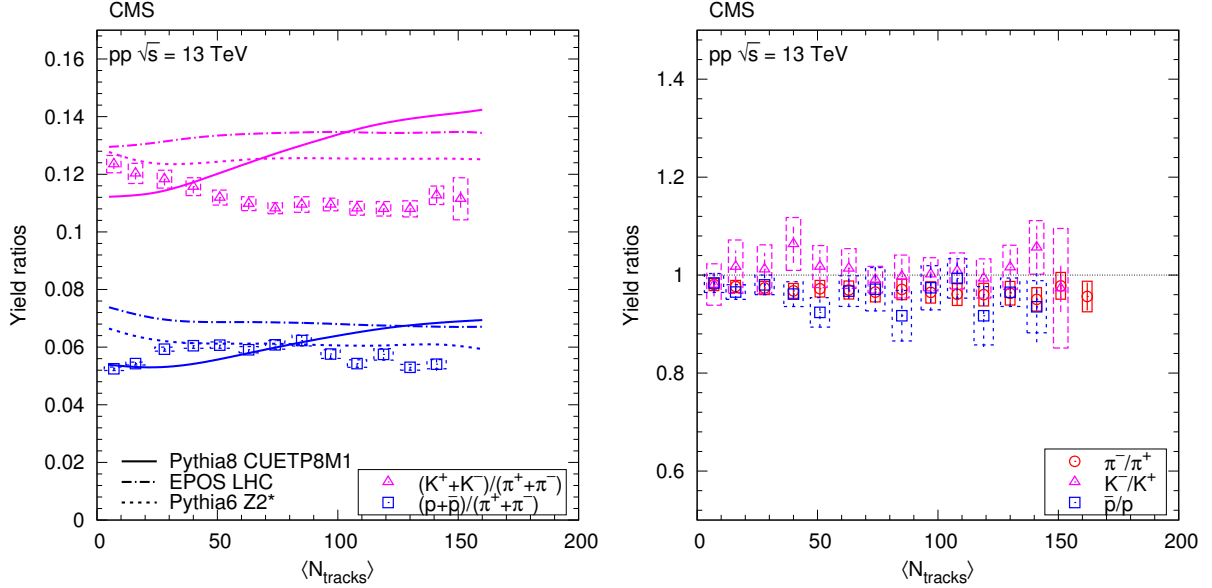


Figure 7: Ratios of particle yields in the range $|y| < 1$ as a function of the corrected track multiplicity for $|\eta| < 2.4$. The K/π and p/π values are shown in the left panel, and opposite-charge ratios are plotted in the right panel. Error bars indicate the uncorrelated combined uncertainties, while boxes show the uncorrelated systematic uncertainties. In the left panel, curves indicate predictions from PYTHIA8, EPOS, and PYTHIA6.

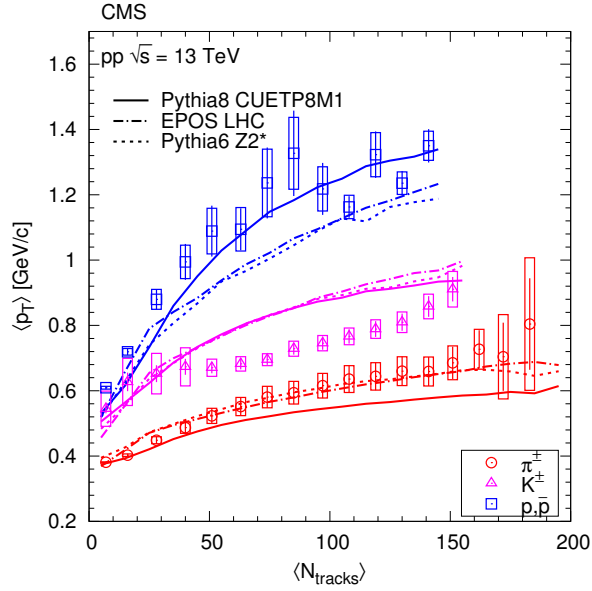


Figure 8: Average transverse momentum of identified charged hadrons (pions, kaons, protons) in the range $|y| < 1$, as functions of the corrected track multiplicity for $|\eta| < 2.4$, computed assuming a Tsallis-Pareto distribution in the unmeasured range. Error bars indicate the uncorrelated combined uncertainties, while boxes show the uncorrelated systematic uncertainties. The fully correlated normalization uncertainty (not shown) is 1.0%. Curves indicate predictions from PYTHIA8, EPOS, and PYTHIA6.

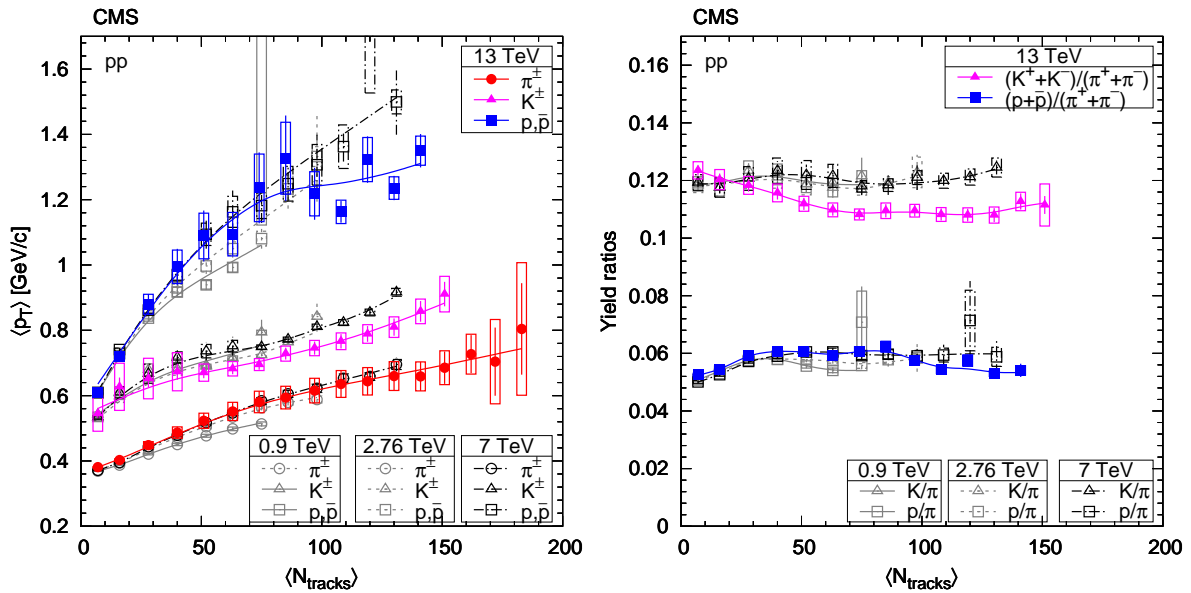


Figure 9: Average transverse momentum of identified charged hadrons (pions, kaons, protons; left panel) and ratios of particle yields (right panel) in the range $|y| < 1$ as functions of the corrected track multiplicity for $|\eta| < 2.4$, for pp collisions at $\sqrt{s} = 13 \text{ TeV}$ (filled symbols) and at lower energies (open symbols) [2]. Both $\langle p_T \rangle$ and yield ratios are computed assuming a Tsallis-Pareto distribution in the unmeasured range. Error bars indicate the uncorrelated combined uncertainties, while boxes show the uncorrelated systematic uncertainties. For $\langle p_T \rangle$ the fully correlated normalization uncertainty (not shown) is 1.0%. In both plots, lines are drawn to guide the eye (gray solid: 0.9 TeV, gray dotted: 2.76 TeV, black dash-dotted: 7 TeV, colored solid: 13 TeV).

slightly decreases with multiplicity.

The ratios of particle yields are displayed as functions of track multiplicity in Fig. 7. The K/π and p/π ratios are relatively flat as a function of $\langle N_{\text{tracks}} \rangle$, and none of the models is able to accurately reproduce the track multiplicity dependence. The ratios of yields of oppositely charged particles are independent of $\langle N_{\text{tracks}} \rangle$ as shown in the right panel of Fig. 7. The average transverse momentum $\langle p_T \rangle$ is shown as a function of multiplicity in Fig. 8. Although PYTHIA8 gives a good description of the (multiplicity integrated) inelastic p_T spectra (Fig. 4), none of the MC event generators reproduces well the multiplicity dependence of $\langle p_T \rangle$ for all particle species. In particular, all generators overestimate the measured values for kaons. Pions are well described by PYTHIA6 and EPOS, while protons are best described by PYTHIA8.

In the lower multiplicity events, with fewer than 50 tracks, we observe a reasonable agreement between the data and the MC generator predictions for the different particle yields. However in higher multiplicity events, the measured kaon (proton) yield is smaller (higher) than predicted by the models. This indicates that the MC parameters that control the strangeness and baryon production as a function of parton multiplicity, need additional fine-tuning.

6.3 Comparisons with lower energy pp data

The comparison of these results with lower-energy pp data taken at various center-of-mass energies (0.9, 2.76, and 7 TeV) [2] is presented in Fig. 9, where the track-multiplicity dependence of $\langle p_T \rangle$ (left) and the particle yield ratios (K/π and p/π , right) are shown. In the previous publication [2], the final results are corrected to a particle-level selection that requires at least

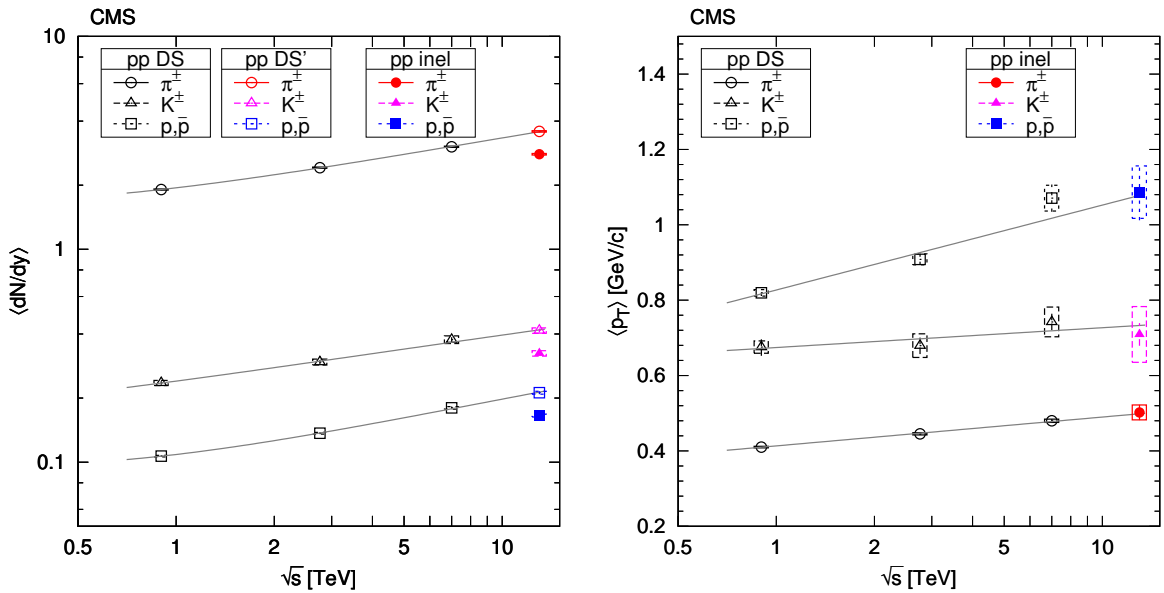


Figure 10: Average rapidity densities $\langle dN/dy \rangle$ (left) and average transverse momenta $\langle p_T \rangle$ (right) for $|y| < 1$ as functions of center-of-mass energy for pp collisions (with data at 0.9, 2.76, and 7 TeV [2]), for charge-averaged pions, kaons, and protons. In the left plot the pp DS' results at 13 TeV have been extrapolated from the inelastic values using simulation. Error bars indicate the uncorrelated combined uncertainties, while boxes show the uncorrelated systematic uncertainties. The curves show parabolic ($\langle dN/dy \rangle$) or linear (for $\langle p_T \rangle$) fits in $\ln s$.

one particle (with proper lifetime $\tau > 10^{-18}$ s) with $E > 3$ GeV in the range $-5 < \eta < -3$ and at least one in the range $3 < \eta < 5$. This selection is referred to as the “double-sided” (DS) selection. Average rapidity densities $\langle dN/dy \rangle$ and average transverse momenta $\langle p_T \rangle$ of charge-averaged pions, kaons, and protons as a function of center-of-mass energy are shown in Fig. 10 corrected to the DS selection (pp DS'). Based on the predictions of the three MC event generators studied, the inelastic $\langle dN/dy \rangle$ result is corrected upwards by 28%, with an additional systematic uncertainty of about 2%. No such correction is applied in the case of $\langle p_T \rangle$, since the inelastic value is close to the DS' one, with a difference of about 1%.

The average p_T increases with particle mass and event multiplicity at all \sqrt{s} , as predicted by all considered event generators. We note that both $\langle p_T \rangle$ and ratios of hadron yields show very similar dependences on the particle multiplicity in the event, independently of the center-of-mass energy of the pp collisions. The \sqrt{s} evolution of the average hadron p_T provides useful information on the so-called “saturation scale” (Q_{sat}) of the gluons in the proton [34]. Minijet-based models such as PYTHIA have an energy-dependent infrared p_T cutoff of the perturbative multiparton cross sections that mimics the power-law evolution of Q_{sat} characteristic of gluon saturation models [35]. In addition, the latter saturation models consistently connect Q_{sat} to the impact parameter of the hadronic collision, thereby providing a natural dependence of $\langle p_T \rangle$ on the final particle multiplicity in the event.

7 Summary

Transverse momentum spectra have been measured for different charged hadron species produced in inelastic pp collisions at $\sqrt{s} = 13$ TeV. Charged pions, kaons, and protons are identified from the energy deposited in the silicon tracker and the reconstructed particle trajectory. The yields of such hadrons at rapidities $|y| < 1$ are studied as a function of the event charged

particle multiplicity measured in the pseudorapidity range $|\eta| < 2.4$. The transverse momentum (p_T) spectra are well described by fits using the Tsallis-Pareto parametrization. The ratios of the yields of oppositely charged particles are close to unity, as expected in the central rapidity region for collisions at this center-of-mass energy. The average p_T is found to increase with particle mass and event multiplicity, and shows features a slow (logarithmiclike or power-law) dependence on \sqrt{s} .

As observed in lower-energy data, the $\langle p_T \rangle$ and the ratios of particle yields are strongly correlated with event particle multiplicity. The PYTHIA8 CUETP8M1 event generator reproduces most features of the measured distributions, which represents a success of the preceding tuning of this model, and EPOS LHC also gives a satisfactory description of several aspects of the data. Although soft QCD effects are intertwined with other effects, the present results could be used to further constrain models of hadron production and to contribute to a better understanding of multiparton interactions, parton hadronization, and final-state effects in high-energy hadron collisions.

Acknowledgments

We congratulate our colleagues in the CERN accelerator departments for the excellent performance of the LHC and thank the technical and administrative staffs at CERN and at other CMS institutes for their contributions to the success of the CMS effort. In addition, we gratefully acknowledge the computing centers and personnel of the Worldwide LHC Computing Grid for delivering so effectively the computing infrastructure essential to our analyses. Finally, we acknowledge the enduring support for the construction and operation of the LHC and the CMS detector provided by the following funding agencies: BMWFW and FWF (Austria); FNRS and FWO (Belgium); CNPq, CAPES, FAPERJ, and FAPESP (Brazil); MES (Bulgaria); CERN; CAS, MoST, and NSFC (China); COLCIENCIAS (Colombia); MSES and CSF (Croatia); RPF (Cyprus); SENESCYT (Ecuador); MoER, ERC IUT, and ERDF (Estonia); Academy of Finland, MEC, and HIP (Finland); CEA and CNRS/IN2P3 (France); BMBF, DFG, and HGF (Germany); GSRT (Greece); OTKA and NIH (Hungary); DAE and DST (India); IPM (Iran); SFI (Ireland); INFN (Italy); MSIP and NRF (Republic of Korea); LAS (Lithuania); MOE and UM (Malaysia); BUAP, CINVESTAV, CONACYT, LNS, SEP, and UASLP-FAI (Mexico); MBIE (New Zealand); PAEC (Pakistan); MSHE and NSC (Poland); FCT (Portugal); JINR (Dubna); MON, RosAtom, RAS, RFBR and RAEP (Russia); MESTD (Serbia); SEIDI, CPAN, PCTI and FEDER (Spain); Swiss Funding Agencies (Switzerland); MST (Taipei); ThEPCenter, IPST, STAR, and NSTDA (Thailand); TUBITAK and TAEK (Turkey); NASU and SFFR (Ukraine); STFC (United Kingdom); DOE and NSF (USA).

Individuals have received support from the Marie-Curie program and the European Research Council and Horizon 2020 Grant, contract No. 675440 (European Union); the Leventis Foundation; the A. P. Sloan Foundation; the Alexander von Humboldt Foundation; the Belgian Federal Science Policy Office; the Fonds pour la Formation à la Recherche dans l’Industrie et dans l’Agriculture (FRIA-Belgium); the Agentschap voor Innovatie door Wetenschap en Technologie (IWT-Belgium); the Ministry of Education, Youth and Sports (MEYS) of the Czech Republic; the Council of Science and Industrial Research, India; the HOMING PLUS program of the Foundation for Polish Science, cofinanced from European Union, Regional Development Fund, the Mobility Plus program of the Ministry of Science and Higher Education, the National Science Center (Poland), contracts Harmonia 2014/14/M/ST2/00428, Opus 2014/13/B/ST2/02543, 2014/15/B/ST2/03998, and 2015/19/B/ST2/02861, Sonata-bis 2012/07/E/ST2/01406; the National Priorities Research Program by Qatar National Research Fund; the Programa Clarín-

COFUND del Principado de Asturias; the Thalis and Aristeia programs cofinanced by EU-ESF and the Greek NSRF; the Rachadapisek Sompot Fund for Postdoctoral Fellowship, Chulalongkorn University and the Chulalongkorn Academic into Its 2nd Century Project Advancement Project (Thailand); and the Welch Foundation, contract C-1845.

References

- [1] LHC Forward Physics Working Group Collaboration, “LHC forward physics”, *J. Phys. G* **43** (2016) 110201, doi:10.1088/0954-3899/43/11/110201, arXiv:1611.05079.
- [2] CMS Collaboration, “Study of the inclusive production of charged pions, kaons, and protons in pp collisions at $\sqrt{s} = 0.9, 2.76$, and 7 TeV ”, *Eur. Phys. J. C* **72** (2012) 2164, doi:10.1140/epjc/s10052-012-2164-1, arXiv:1207.4724.
- [3] ALICE Collaboration, “Measurement of pion, kaon and proton production in proton-proton collisions at $\sqrt{s} = 7 \text{ TeV}$ ”, *Eur. Phys. J. C* **75** (2015) 226, doi:10.1140/epjc/s10052-015-3422-9, arXiv:1504.00024.
- [4] D. d’Enterria et al., “Constraints from the first LHC data on hadronic event generators for ultra-high energy cosmic-ray physics”, *Astropart. Phys.* **35** (2011) 98, doi:10.1016/j.astropartphys.2011.05.002, arXiv:1101.5596.
- [5] CMS Collaboration, “Nuclear Effects on the Transverse Momentum Spectra of Charged Particles in pPb Collisions at $\sqrt{s_{\text{NN}}} = 5.02 \text{ TeV}$ ”, *Eur. Phys. J. C* **75** (2015) 237, doi:10.1140/epjc/s10052-015-3435-4, arXiv:1502.05387.
- [6] CMS Collaboration, “Charged-particle nuclear modification factors in PbPb and pPb collisions at $\sqrt{s_{\text{NN}}} = 5.02 \text{ TeV}$ ”, *JHEP* **04** (2017) 039, doi:10.1007/JHEP04(2017)039, arXiv:1611.01664.
- [7] ALICE Collaboration, “Centrality dependence of the nuclear modification factor of charged pions, kaons, and protons in Pb-Pb collisions at $\sqrt{s_{\text{NN}}} = 2.76 \text{ TeV}$ ”, *Phys. Rev. C* **93** (2016) 034913, doi:10.1103/PhysRevC.93.034913, arXiv:1506.07287.
- [8] ALICE Collaboration, “Pion, kaon, and proton production in central Pb–Pb collisions at $\sqrt{s_{\text{NN}}} = 2.76 \text{ TeV}$ ”, *Phys. Rev. Lett.* **109** (2012) 252301, doi:10.1103/PhysRevLett.109.252301, arXiv:1208.1974.
- [9] ALICE Collaboration, “Production of charged pions, kaons and protons at large transverse momenta in pp and Pb-d-Pb collisions at $\sqrt{s_{\text{NN}}} = 2.76 \text{ TeV}$ ”, *Phys. Lett. B* **736** (2014) 196, doi:10.1016/j.physletb.2014.07.011, arXiv:1401.1250.
- [10] CMS Collaboration, “Study of the production of charged pions, kaons, and protons in pPb collisions at $\sqrt{s_{\text{NN}}} = 5.02 \text{ TeV}$ ”, *Eur. Phys. J. C* **74** (2014) 2847, doi:10.1140/epjc/s10052-014-2847-x, arXiv:1307.3442.
- [11] ALICE Collaboration, “Production of pions, kaons and protons in pp collisions at $\sqrt{s} = 900 \text{ GeV}$ with ALICE at the LHC”, *Eur. Phys. J. C* **71** (2011) 1, doi:10.1140/epjc/s10052-011-1655-9, arXiv:1101.4110.
- [12] CMS Collaboration, “The CMS experiment at the CERN LHC”, *JINST* **3** (2008) S08004, doi:10.1088/1748-0221/3/08/S08004.
- [13] T. Sjöstrand, S. Mrenna, and P. Z. Skands, “PYTHIA 6.4 physics and manual”, *JHEP* **05** (2006) 026, doi:10.1088/1126-6708/2006/05/026, arXiv:hep-ph/0603175.
- [14] T. Sjöstrand, S. Mrenna, and P. Z. Skands, “A brief introduction to PYTHIA 8.1”, *Comput. Phys. Commun.* **178** (2008) 852, doi:10.1016/j.cpc.2008.01.036, arXiv:0710.3820.

- [15] K. Werner, F.-M. Liu, and T. Pierog, “Parton ladder splitting and the rapidity dependence of transverse momentum spectra in deuteron-gold collisions at RHIC”, *Phys. Rev. C* **74** (2006) 044902, doi:[10.1103/PhysRevC.74.044902](https://doi.org/10.1103/PhysRevC.74.044902), arXiv:[hep-ph/0506232](https://arxiv.org/abs/hep-ph/0506232).
- [16] CMS Collaboration, “Event generator tunes obtained from underlying event and multiparton scattering measurements”, *Eur. Phys. J. C* **76** (2016) 155, doi:[10.1140/epjc/s10052-016-3988-x](https://doi.org/10.1140/epjc/s10052-016-3988-x), arXiv:[1512.00815](https://arxiv.org/abs/1512.00815).
- [17] V. N. Gribov, “A Reggeon Diagram Technique”, *Sov. Phys. JETP* **26** (1968) 414. [Zh. Eksp. Teor. Fiz. 53, 654 (1967)].
- [18] T. Pierog et al., “EPOS LHC: Test of collective hadronization with data measured at the CERN Large Hadron Collider”, *Phys. Rev. C* **92** (2015) 034906, doi:[10.1103/PhysRevC.92.034906](https://doi.org/10.1103/PhysRevC.92.034906), arXiv:[1306.0121](https://arxiv.org/abs/1306.0121).
- [19] CMS Collaboration, “Transverse momentum and pseudorapidity distributions of charged hadrons in pp collisions at $\sqrt{s} = 0.9$ and 2.36 TeV”, *JHEP* **02** (2010) 041, doi:[10.1007/JHEP02\(2010\)041](https://doi.org/10.1007/JHEP02(2010)041), arXiv:[1002.0621](https://arxiv.org/abs/1002.0621).
- [20] S. Agostinelli et al., “Geant4 — a simulation toolkit”, *Nucl. Instrum. Meth. A* **506** (2003) 250, doi:[10.1016/S0168-9002\(03\)01368-8](https://doi.org/10.1016/S0168-9002(03)01368-8).
- [21] F. Siklér, “Low p_t hadronic physics with CMS”, *Int. J. Mod. Phys. E* **16** (2007) 1819, doi:[10.1142/S0218301307007052](https://doi.org/10.1142/S0218301307007052), arXiv:[physics/0702193](https://arxiv.org/abs/physics/0702193).
- [22] CMS Collaboration, “Transverse-momentum and pseudorapidity distributions of charged hadrons in pp collisions at $\sqrt{s} = 7$ TeV”, *Phys. Rev. Lett.* **105** (2010) 022002, doi:[10.1103/PhysRevLett.105.022002](https://doi.org/10.1103/PhysRevLett.105.022002), arXiv:[1005.3299](https://arxiv.org/abs/1005.3299).
- [23] F. Siklér, “Study of clustering methods to improve primary vertex finding for collider detectors”, *Nucl. Instrum. Meth. A* **621** (2010) 526, doi:[10.1016/j.nima.2010.04.058](https://doi.org/10.1016/j.nima.2010.04.058), arXiv:[0911.2767](https://arxiv.org/abs/0911.2767).
- [24] F. Siklér, “A parametrisation of the energy loss distributions of charged particles and its applications for silicon detectors”, *Nucl. Instrum. Meth. A* **691** (2012) 16, doi:[10.1016/j.nima.2012.06.064](https://doi.org/10.1016/j.nima.2012.06.064), arXiv:[1111.3213](https://arxiv.org/abs/1111.3213).
- [25] Particle Data Group Collaboration, “Review of particle physics”, *Chin. Phys. C* **40** (2016) 100001, doi:[10.1088/1674-1137/40/10/100001](https://doi.org/10.1088/1674-1137/40/10/100001).
- [26] A. N. Tikhonov, “Solution of incorrectly formulated problems and the regularization method”, *Soviet Math. Dokl.* **4** (1963) 1035.
- [27] CMS Collaboration, “Strange particle production in pp collisions at $\sqrt{s} = 0.9$ and 7 TeV”, *JHEP* **05** (2011) 064, doi:[10.1007/JHEP05\(2011\)064](https://doi.org/10.1007/JHEP05(2011)064), arXiv:[1102.4282](https://arxiv.org/abs/1102.4282).
- [28] C. Tsallis, “Possible generalization of Boltzmann-Gibbs statistics”, *J. Stat. Phys.* **52** (1988) 479, doi:[10.1007/BF01016429](https://doi.org/10.1007/BF01016429).
- [29] T. S. Biró, G. Purcsel, and K. Ürmössy, “Non-extensive approach to quark matter”, *Eur. Phys. J. A* **40** (2009) 325, doi:[10.1140/epja/i2009-10806-6](https://doi.org/10.1140/epja/i2009-10806-6), arXiv:[0812.2104](https://arxiv.org/abs/0812.2104).
- [30] CMS Collaboration, “Observation of long-range near-side angular correlations in proton-proton collisions at the LHC”, *JHEP* **09** (2010) 091, doi:[10.1007/JHEP09\(2010\)091](https://doi.org/10.1007/JHEP09(2010)091), arXiv:[1009.4122](https://arxiv.org/abs/1009.4122).

- [31] CMS Collaboration, “Observation of long-range near-side angular correlations in proton-lead collisions at the LHC”, *Phys. Lett. B* **718** (2013) 795,
[doi:10.1016/j.physletb.2012.11.025](https://doi.org/10.1016/j.physletb.2012.11.025), arXiv:1210.5482.
- [32] ALICE Collaboration, “Long-range angular correlations on the near and away side in p-Pb collisions at $\sqrt{s_{NN}} = 5.02$ TeV”, *Phys. Lett. B* **719** (2013) 29,
[doi:10.1016/j.physletb.2013.01.012](https://doi.org/10.1016/j.physletb.2013.01.012), arXiv:1212.2001.
- [33] ATLAS Collaboration, “Observation of associated near-side and away-side long-range correlations in $\sqrt{s_{NN}} = 5.02$ TeV proton-lead collisions with the ATLAS detector”, *Phys. Rev. Lett.* **110** (2013) 182302, [doi:10.1103/PhysRevLett.110.182302](https://doi.org/10.1103/PhysRevLett.110.182302), arXiv:1212.5198.
- [34] D. d’Enterria and T. Pierog, “Global properties of proton-proton collisions at $\sqrt{s} = 100$ TeV”, *JHEP* **08** (2016) 170, [doi:10.1007/JHEP08\(2016\)170](https://doi.org/10.1007/JHEP08(2016)170), arXiv:1604.08536.
- [35] L. McLerran, M. Praszalowicz, and B. Schenke, “Transverse momentum of protons, pions and kaons in high multiplicity pp and pA collisions: Evidence for the color glass condensate?”, *Nucl. Phys. A* **916** (2013) 210,
[doi:10.1016/j.nuclphysa.2013.08.008](https://doi.org/10.1016/j.nuclphysa.2013.08.008), arXiv:1306.2350.

A The CMS Collaboration

Yerevan Physics Institute, Yerevan, Armenia

A.M. Sirunyan, A. Tumasyan

Institut für Hochenergiephysik, Wien, Austria

W. Adam, E. Asilar, T. Bergauer, J. Brandstetter, E. Brondolin, M. Dragicevic, J. Erö, M. Flechl, M. Friedl, R. Frühwirth¹, V.M. Ghete, C. Hartl, N. Hörmann, J. Hrubec, M. Jeitler¹, A. König, I. Krätschmer, D. Liko, T. Matsushita, I. Mikulec, D. Rabady, N. Rad, B. Rahbaran, H. Rohringer, J. Schieck¹, J. Strauss, W. Waltenberger, C.-E. Wulz¹

Institute for Nuclear Problems, Minsk, Belarus

O. Dvornikov, V. Makarenko, V. Mossolov, J. Suarez Gonzalez, V. Zykunov

National Centre for Particle and High Energy Physics, Minsk, Belarus

N. Shumeiko

Universiteit Antwerpen, Antwerpen, Belgium

S. Alderweireldt, E.A. De Wolf, X. Janssen, J. Lauwers, M. Van De Klundert, H. Van Haevermaet, P. Van Mechelen, N. Van Remortel, A. Van Spilbeeck

Vrije Universiteit Brussel, Brussel, Belgium

S. Abu Zeid, F. Blekman, J. D'Hondt, N. Daci, I. De Bruyn, K. Deroover, S. Lowette, S. Moortgat, L. Moreels, A. Olbrechts, Q. Python, K. Skovpen, S. Tavernier, W. Van Doninck, P. Van Mulders, I. Van Parijs

Université Libre de Bruxelles, Bruxelles, Belgium

H. Brun, B. Clerbaux, G. De Lentdecker, H. Delannoy, G. Fasanella, L. Favart, R. Goldouzian, A. Grebenyuk, G. Karapostoli, T. Lenzi, A. Léonard, J. Luetic, T. Maerschalk, A. Marinov, A. Randle-conde, T. Seva, C. Vander Velde, P. Vanlaer, D. Vannerom, R. Yonamine, F. Zenoni, F. Zhang²

Ghent University, Ghent, Belgium

A. Cimmino, T. Cornelis, D. Dobur, A. Fagot, M. Gul, I. Khvastunov, D. Poyraz, S. Salva, R. Schöfbeck, M. Tytgat, W. Van Driessche, E. Yazgan, N. Zaganidis

Université Catholique de Louvain, Louvain-la-Neuve, Belgium

H. Bakhshiansohi, C. Beluffi³, O. Bondu, S. Brochet, G. Bruno, A. Caudron, S. De Visscher, C. Delaere, M. Delcourt, B. Francois, A. Giannanco, A. Jafari, M. Komm, G. Krintiras, V. Lemaitre, A. Magitteri, A. Mertens, M. Musich, K. Piotrzkowski, L. Quertenmont, M. Selvaggi, M. Vidal Marono, S. Wertz

Université de Mons, Mons, Belgium

N. Belyi

Centro Brasileiro de Pesquisas Fisicas, Rio de Janeiro, Brazil

W.L. Aldá Júnior, F.L. Alves, G.A. Alves, L. Brito, C. Hensel, A. Moraes, M.E. Pol, P. Rebello Teles

Universidade do Estado do Rio de Janeiro, Rio de Janeiro, Brazil

E. Belchior Batista Das Chagas, W. Carvalho, J. Chinellato⁴, A. Custódio, E.M. Da Costa, G.G. Da Silveira⁵, D. De Jesus Damiao, C. De Oliveira Martins, S. Fonseca De Souza, L.M. Huertas Guativa, H. Malbouisson, D. Matos Figueiredo, C. Mora Herrera, L. Mundim, H. Nogima, W.L. Prado Da Silva, A. Santoro, A. Sznajder, E.J. Tonelli Manganote⁴, F. Torres Da Silva De Araujo, A. Vilela Pereira

Universidade Estadual Paulista ^a, Universidade Federal do ABC ^b, São Paulo, Brazil
 S. Ahuja^a, C.A. Bernardes^a, S. Dogra^a, T.R. Fernandez Perez Tomei^a, E.M. Gregores^b,
 P.G. Mercadante^b, C.S. Moon^a, S.F. Novaes^a, Sandra S. Padula^a, D. Romero Abad^b, J.C. Ruiz
 Vargas^a

Institute for Nuclear Research and Nuclear Energy, Sofia, Bulgaria

A. Aleksandrov, R. Hadjiiska, P. Iaydjiev, M. Rodozov, S. Stoykova, G. Sultanov, M. Vutova

University of Sofia, Sofia, Bulgaria

A. Dimitrov, I. Glushkov, L. Litov, B. Pavlov, P. Petkov

Beihang University, Beijing, China

W. Fang⁶

Institute of High Energy Physics, Beijing, China

M. Ahmad, J.G. Bian, G.M. Chen, H.S. Chen, M. Chen, Y. Chen⁷, T. Cheng, C.H. Jiang,
 D. Leggat, Z. Liu, F. Romeo, M. Ruan, S.M. Shaheen, A. Spiezja, J. Tao, C. Wang, Z. Wang,
 H. Zhang, J. Zhao

State Key Laboratory of Nuclear Physics and Technology, Peking University, Beijing, China

Y. Ban, G. Chen, Q. Li, S. Liu, Y. Mao, S.J. Qian, D. Wang, Z. Xu

Universidad de Los Andes, Bogota, Colombia

C. Avila, A. Cabrera, L.F. Chaparro Sierra, C. Florez, J.P. Gomez, C.F. González Hernández,
 J.D. Ruiz Alvarez⁸, J.C. Sanabria

**University of Split, Faculty of Electrical Engineering, Mechanical Engineering and Naval
 Architecture, Split, Croatia**

N. Godinovic, D. Lelas, I. Puljak, P.M. Ribeiro Cipriano, T. Sculac

University of Split, Faculty of Science, Split, Croatia

Z. Antunovic, M. Kovac

Institute Rudjer Boskovic, Zagreb, Croatia

V. Brigljevic, D. Ferencek, K. Kadija, B. Mesic, T. Susa

University of Cyprus, Nicosia, Cyprus

M.W. Ather, A. Attikis, G. Mavromanolakis, J. Mousa, C. Nicolaou, F. Ptochos, P.A. Razis,
 H. Rykaczewski

Charles University, Prague, Czech Republic

M. Finger⁹, M. Finger Jr.⁹

Universidad San Francisco de Quito, Quito, Ecuador

E. Carrera Jarrin

**Academy of Scientific Research and Technology of the Arab Republic of Egypt, Egyptian
 Network of High Energy Physics, Cairo, Egypt**

A.A. Abdelalim^{10,11}, Y. Mohammed¹², E. Salama^{13,14}

National Institute of Chemical Physics and Biophysics, Tallinn, Estonia

M. Kadastik, L. Perrini, M. Raidal, A. Tiko, C. Veelken

Department of Physics, University of Helsinki, Helsinki, Finland

P. Eerola, J. Pekkanen, M. Voutilainen

Helsinki Institute of Physics, Helsinki, Finland

J. Härkönen, T. Järvinen, V. Karimäki, R. Kinnunen, T. Lampén, K. Lassila-Perini, S. Lehti, T. Lindén, P. Luukka, J. Tuominiemi, E. Tuovinen, L. Wendland

Lappeenranta University of Technology, Lappeenranta, Finland

J. Talvitie, T. Tuuva

IRFU, CEA, Université Paris-Saclay, Gif-sur-Yvette, France

M. Besancon, F. Couderc, M. Dejardin, D. Denegri, B. Fabbro, J.L. Faure, C. Favaro, F. Ferri, S. Ganjour, S. Ghosh, A. Givernaud, P. Gras, G. Hamel de Monchenault, P. Jarry, I. Kucher, E. Locci, M. Machet, J. Malcles, J. Rander, A. Rosowsky, M. Titov

Laboratoire Leprince-Ringuet, Ecole polytechnique, CNRS/IN2P3, Université Paris-Saclay, Palaiseau, France

A. Abdulsalam, I. Antropov, S. Baffioni, F. Beaudette, P. Busson, L. Cadamuro, E. Chapon, C. Charlot, O. Davignon, R. Granier de Cassagnac, M. Jo, S. Lisniak, P. Miné, M. Nguyen, C. Ochando, G. Ortona, P. Paganini, P. Pigard, S. Regnard, R. Salerno, Y. Sirois, A.G. Stahl Leiton, T. Strebler, Y. Yilmaz, A. Zabi, A. Zghiche

Université de Strasbourg, CNRS, IPHC UMR 7178, F-67000 Strasbourg, France

J.-L. Agram¹⁵, J. Andrea, A. Aubin, D. Bloch, J.-M. Brom, M. Buttignol, E.C. Chabert, N. Chanon, C. Collard, E. Conte¹⁵, X. Coubez, J.-C. Fontaine¹⁵, D. Gelé, U. Goerlach, A.-C. Le Bihan, P. Van Hove

Centre de Calcul de l’Institut National de Physique Nucléaire et de Physique des Particules, CNRS/IN2P3, Villeurbanne, France

S. Gadrat

Université de Lyon, Université Claude Bernard Lyon 1, CNRS-IN2P3, Institut de Physique Nucléaire de Lyon, Villeurbanne, France

S. Beauceron, C. Bernet, G. Boudoul, C.A. Carrillo Montoya, R. Chierici, D. Contardo, B. Courbon, P. Depasse, H. El Mamouni, J. Fay, S. Gascon, M. Gouzevitch, G. Grenier, B. Ille, F. Lagarde, I.B. Laktineh, M. Lethuillier, L. Mirabito, A.L. Pequegnot, S. Perries, A. Popov¹⁶, V. Sordini, M. Vander Donckt, P. Verdier, S. Viret

Georgian Technical University, Tbilisi, Georgia

T. Toriashvili¹⁷

Tbilisi State University, Tbilisi, Georgia

Z. Tsamalaidze⁹

RWTH Aachen University, I. Physikalisches Institut, Aachen, Germany

C. Autermann, S. Beranek, L. Feld, M.K. Kiesel, K. Klein, M. Lipinski, M. Preuten, C. Schomakers, J. Schulz, T. Verlage

RWTH Aachen University, III. Physikalisches Institut A, Aachen, Germany

A. Albert, M. Brodski, E. Dietz-Laursonn, D. Duchardt, M. Endres, M. Erdmann, S. Erdweg, T. Esch, R. Fischer, A. Güth, M. Hamer, T. Hebbeker, C. Heidemann, K. Hoepfner, S. Knutzen, M. Merschmeyer, A. Meyer, P. Millet, S. Mukherjee, M. Olszewski, K. Padeken, T. Pook, M. Radziej, H. Reithler, M. Rieger, F. Scheuch, L. Sonnenschein, D. Teyssier, S. Thüer

RWTH Aachen University, III. Physikalisches Institut B, Aachen, Germany

V. Cherepanov, G. Flügge, B. Kargoll, T. Kress, A. Künsken, J. Lingemann, T. Müller, A. Nehrkorn, A. Nowack, C. Pistone, O. Pooth, A. Stahl¹⁸

Deutsches Elektronen-Synchrotron, Hamburg, Germany

M. Aldaya Martin, T. Arndt, C. Asawatangtrakuldee, K. Beernaert, O. Behnke, U. Behrens, A.A. Bin Anuar, K. Borras¹⁹, A. Campbell, P. Connor, C. Contreras-Campana, F. Costanza, C. Diez Pardos, G. Dolinska, G. Eckerlin, D. Eckstein, T. Eichhorn, E. Eren, E. Gallo²⁰, J. Garay Garcia, A. Geiser, A. Gizhko, J.M. Grados Luyando, A. Grohsjean, P. Gunnellini, A. Harb, J. Hauk, M. Hempel²¹, H. Jung, A. Kalogeropoulos, O. Karacheban²¹, M. Kasemann, J. Keaveney, C. Kleinwort, I. Korol, D. Krücker, W. Lange, A. Lelek, T. Lenz, J. Leonard, K. Lipka, A. Lobanov, W. Lohmann²¹, R. Mankel, I.-A. Melzer-Pellmann, A.B. Meyer, G. Mittag, J. Mnich, A. Mussgiller, D. Pitzl, R. Placakyte, A. Raspareza, B. Roland, M.Ö. Sahin, P. Saxena, T. Schoerner-Sadenius, S. Spannagel, N. Stefanik, G.P. Van Onsem, R. Walsh, C. Wissing

University of Hamburg, Hamburg, Germany

V. Blobel, M. Centis Vignali, A.R. Draeger, T. Dreyer, E. Garutti, D. Gonzalez, J. Haller, M. Hoffmann, A. Junkes, R. Klanner, R. Kogler, N. Kovalchuk, T. Lapsien, I. Marchesini, D. Marconi, M. Meyer, M. Niedziela, D. Nowatschin, F. Pantaleo¹⁸, T. Peiffer, A. Perieanu, C. Scharf, P. Schleper, A. Schmidt, S. Schumann, J. Schwandt, H. Stadie, G. Steinbrück, F.M. Stober, M. Stöver, H. Tholen, D. Troendle, E. Usai, L. Vanelderen, A. Vanhoefer, B. Vormwald

Institut für Experimentelle Kernphysik, Karlsruhe, Germany

M. Akbiyik, C. Barth, S. Baur, C. Baus, J. Berger, E. Butz, R. Caspart, T. Chwalek, F. Colombo, W. De Boer, A. Dierlamm, S. Fink, B. Freund, R. Friese, M. Giffels, A. Gilbert, P. Goldenzweig, D. Haitz, F. Hartmann¹⁸, S.M. Heindl, U. Husemann, F. Kassel¹⁸, I. Katkov¹⁶, S. Kudella, H. Mildner, M.U. Mozer, Th. Müller, M. Plagge, G. Quast, K. Rabbertz, S. Röcker, F. Roscher, M. Schröder, I. Shvetsov, G. Sieber, H.J. Simonis, R. Ulrich, S. Wayand, M. Weber, T. Weiler, S. Williamson, C. Wöhrmann, R. Wolf

Institute of Nuclear and Particle Physics (INPP), NCSR Demokritos, Aghia Paraskevi, Greece

G. Anagnostou, G. Daskalakis, T. Geralis, V.A. Giakoumopoulou, A. Kyriakis, D. Loukas, I. Topsis-Giotis

National and Kapodistrian University of Athens, Athens, Greece

S. Kesisoglou, A. Panagiotou, N. Saoulidou, E. Tziaferi

University of Ioánnina, Ioánnina, Greece

I. Evangelou, G. Flouris, C. Foudas, P. Kokkas, N. Loukas, N. Manthos, I. Papadopoulos, E. Paradas

MTA-ELTE Lendület CMS Particle and Nuclear Physics Group, Eötvös Loránd University, Budapest, Hungary

N. Filipovic, G. Pasztor

Wigner Research Centre for Physics, Budapest, Hungary

G. Bencze, C. Hajdu, D. Horvath²², F. Sikler, V. Veszpremi, G. Vesztregombi²³, A.J. Zsigmond

Institute of Nuclear Research ATOMKI, Debrecen, Hungary

N. Beni, S. Czellar, J. Karancsi²⁴, A. Makovec, J. Molnar, Z. Szillasi

Institute of Physics, University of Debrecen, Debrecen, Hungary

M. Bartók²³, P. Raics, Z.L. Trocsanyi, B. Ujvari

Indian Institute of Science (IISc), Bangalore, India

J.R. Komaragiri

National Institute of Science Education and Research, Bhubaneswar, India

S. Bahinipati²⁵, S. Bhowmik²⁶, S. Choudhury²⁷, P. Mal, K. Mandal, A. Nayak²⁸, D.K. Sahoo²⁵, N. Sahoo, S.K. Swain

Panjab University, Chandigarh, India

S. Bansal, S.B. Beri, V. Bhatnagar, U. Bhawandep, R. Chawla, A.K. Kalsi, A. Kaur, M. Kaur, R. Kumar, P. Kumari, A. Mehta, M. Mittal, J.B. Singh, G. Walia

University of Delhi, Delhi, India

Ashok Kumar, A. Bhardwaj, B.C. Choudhary, R.B. Garg, S. Keshri, S. Malhotra, M. Naimuddin, K. Ranjan, R. Sharma, V. Sharma

Saha Institute of Nuclear Physics, HBNI, Kolkata, India

R. Bhattacharya, S. Bhattacharya, K. Chatterjee, S. Dey, S. Dutt, S. Dutta, S. Ghosh, N. Majumdar, A. Modak, K. Mondal, S. Mukhopadhyay, S. Nandan, A. Purohit, A. Roy, D. Roy, S. Roy Chowdhury, S. Sarkar, M. Sharan, S. Thakur

Indian Institute of Technology Madras, Madras, India

P.K. Behera

Bhabha Atomic Research Centre, Mumbai, India

R. Chudasama, D. Dutta, V. Jha, V. Kumar, A.K. Mohanty¹⁸, P.K. Netrakanti, L.M. Pant, P. Shukla, A. Topkar

Tata Institute of Fundamental Research-A, Mumbai, India

T. Aziz, S. Dugad, G. Kole, B. Mahakud, S. Mitra, G.B. Mohanty, B. Parida, N. Sur, B. Sutar

Tata Institute of Fundamental Research-B, Mumbai, India

S. Banerjee, R.K. Dewanjee, S. Ganguly, M. Guchait, Sa. Jain, S. Kumar, M. Maity²⁶, G. Majumder, K. Mazumdar, T. Sarkar²⁶, N. Wickramage²⁹

Indian Institute of Science Education and Research (IISER), Pune, India

S. Chauhan, S. Dube, V. Hegde, A. Kapoor, K. Kotheendar, S. Pandey, A. Rane, S. Sharma

Institute for Research in Fundamental Sciences (IPM), Tehran, Iran

S. Chenarani³⁰, E. Eskandari Tadavani, S.M. Etesami³⁰, M. Khakzad, M. Mohammadi Najafabadi, M. Naseri, S. Pakhtinat Mehdiabadi³¹, F. Rezaei Hosseiniabadi, B. Safarzadeh³², M. Zeinali

University College Dublin, Dublin, Ireland

M. Felcini, M. Grunewald

INFN Sezione di Bari ^a, Università di Bari ^b, Politecnico di Bari ^c, Bari, Italy

M. Abbrescia^{a,b}, C. Calabria^{a,b}, C. Caputo^{a,b}, A. Colaleo^a, D. Creanza^{a,c}, L. Cristella^{a,b}, N. De Filippis^{a,c}, M. De Palma^{a,b}, L. Fiore^a, G. Iaselli^{a,c}, G. Maggi^{a,c}, M. Maggi^a, G. Minnello^{a,b}, S. My^{a,b}, S. Nuzzo^{a,b}, A. Pompili^{a,b}, G. Pugliese^{a,c}, R. Radogna^{a,b}, A. Ranieri^a, G. Selvaggi^{a,b}, A. Sharma^a, L. Silvestris^{a,18}, R. Venditti^{a,b}, P. Verwilligen^a

INFN Sezione di Bologna ^a, Università di Bologna ^b, Bologna, Italy

G. Abbiendi^a, C. Battilana, D. Bonacorsi^{a,b}, S. Braibant-Giacomelli^{a,b}, L. Brigliadori^{a,b}, R. Campanini^{a,b}, P. Capiluppi^{a,b}, A. Castro^{a,b}, F.R. Cavallo^a, S.S. Chhibra^{a,b}, G. Codispoti^{a,b}, M. Cuffiani^{a,b}, G.M. Dallavalle^a, F. Fabbri^a, A. Fanfani^{a,b}, D. Fasanella^{a,b}, P. Giacomelli^a, C. Grandi^a, L. Guiducci^{a,b}, S. Marcellini^a, G. Masetti^a, A. Montanari^a, F.L. Navarria^{a,b}, A. Perrotta^a, A.M. Rossi^{a,b}, T. Rovelli^{a,b}, G.P. Siroli^{a,b}, N. Tosi^{a,b,18}

INFN Sezione di Catania ^a, Università di Catania ^b, Catania, ItalyS. Albergo^{a,b}, S. Costa^{a,b}, A. Di Mattia^a, F. Giordano^{a,b}, R. Potenza^{a,b}, A. Tricomi^{a,b}, C. Tuve^{a,b}**INFN Sezione di Firenze ^a, Università di Firenze ^b, Firenze, Italy**G. Barbagli^a, V. Ciulli^{a,b}, C. Civinini^a, R. D'Alessandro^{a,b}, E. Focardi^{a,b}, P. Lenzi^{a,b}, M. Meschini^a, S. Paoletti^a, L. Russo^{a,33}, G. Sguazzoni^a, D. Strom^a, L. Viliani^{a,b,18}**INFN Laboratori Nazionali di Frascati, Frascati, Italy**L. Benussi, S. Bianco, F. Fabbri, D. Piccolo, F. Primavera¹⁸**INFN Sezione di Genova ^a, Università di Genova ^b, Genova, Italy**V. Calvelli^{a,b}, F. Ferro^a, M.R. Monge^{a,b}, E. Robutti^a, S. Tosi^{a,b}**INFN Sezione di Milano-Bicocca ^a, Università di Milano-Bicocca ^b, Milano, Italy**L. Brianza^{a,b,18}, F. Brivio^{a,b}, V. Ciriolo, M.E. Dinardo^{a,b}, S. Fiorendi^{a,b,18}, S. Gennai^a, A. Ghezzi^{a,b}, P. Govoni^{a,b}, M. Malberti^{a,b}, S. Malvezzi^a, R.A. Manzoni^{a,b}, D. Menasce^a, L. Moroni^a, M. Paganoni^{a,b}, D. Pedrini^a, S. Pigazzini^{a,b}, S. Ragazzi^{a,b}, T. Tabarelli de Fatis^{a,b}**INFN Sezione di Napoli ^a, Università di Napoli 'Federico II' ^b, Napoli, Italy, Università della Basilicata ^c, Potenza, Italy, Università G. Marconi ^d, Roma, Italy**S. Buontempo^a, N. Cavallo^{a,c}, G. De Nardo, S. Di Guida^{a,d,18}, F. Fabozzi^{a,c}, F. Fienga^{a,b}, A.O.M. Iorio^{a,b}, L. Lista^a, S. Meola^{a,d,18}, P. Paolucci^{a,18}, C. Sciacca^{a,b}, F. Thyssen^a**INFN Sezione di Padova ^a, Università di Padova ^b, Padova, Italy, Università di Trento ^c, Trento, Italy**P. Azzi^{a,18}, N. Bacchetta^a, L. Benato^{a,b}, D. Bisello^{a,b}, A. Boletti^{a,b}, R. Carlin^{a,b}, A. Carvalho Antunes De Oliveira^{a,b}, P. Checchia^a, M. Dall'Osso^{a,b}, P. De Castro Manzano^a, T. Dorigo^a, U. Dosselli^a, F. Gasparini^{a,b}, U. Gasparini^{a,b}, A. Gozzelino^a, S. Lacaprara^a, M. Margoni^{a,b}, A.T. Meneguzzo^{a,b}, J. Pazzini^{a,b}, N. Pozzobon^{a,b}, P. Ronchese^{a,b}, F. Simonetto^{a,b}, E. Torassa^a, M. Zanetti^{a,b}, P. Zotto^{a,b}, G. Zumerle^{a,b}**INFN Sezione di Pavia ^a, Università di Pavia ^b, Pavia, Italy**A. Braghieri^a, F. Fallavollita^{a,b}, A. Magnani^{a,b}, P. Montagna^{a,b}, S.P. Ratti^{a,b}, V. Re^a, C. Riccardi^{a,b}, P. Salvini^a, I. Vai^{a,b}, P. Vitulo^{a,b}**INFN Sezione di Perugia ^a, Università di Perugia ^b, Perugia, Italy**L. Alunni Solestizi^{a,b}, G.M. Bilei^a, D. Ciangottini^{a,b}, L. Fanò^{a,b}, P. Lariccia^{a,b}, R. Leonardi^{a,b}, G. Mantovani^{a,b}, V. Mariani^{a,b}, M. Menichelli^a, A. Saha^a, A. Santocchia^{a,b}**INFN Sezione di Pisa ^a, Università di Pisa ^b, Scuola Normale Superiore di Pisa ^c, Pisa, Italy**K. Androsov^{a,33}, P. Azzurri^{a,18}, G. Bagliesi^a, J. Bernardini^a, T. Boccali^a, R. Castaldi^a, M.A. Ciocci^{a,33}, R. Dell'Orso^a, S. Donato^{a,c}, G. Fedi, A. Giassi^a, M.T. Grippo^{a,33}, F. Ligabue^{a,c}, T. Lomtadze^a, L. Martini^{a,b}, A. Messineo^{a,b}, F. Palla^a, A. Rizzi^{a,b}, A. Savoy-Navarro^{a,34}, P. Spagnolo^a, R. Tenchini^a, G. Tonelli^{a,b}, A. Venturi^a, P.G. Verdini^a**INFN Sezione di Roma ^a, Sapienza Università di Roma ^b, Rome, Italy**L. Barone^{a,b}, F. Cavallari^a, M. Cipriani^{a,b}, D. Del Re^{a,b,18}, M. Diemoz^a, S. Gelli^{a,b}, E. Longo^{a,b}, F. Margaroli^{a,b}, B. Marzocchi^{a,b}, P. Meridiani^a, G. Organtini^{a,b}, R. Paramatti^{a,b}, F. Preiato^{a,b}, S. Rahatlou^{a,b}, C. Rovelli^a, F. Santanastasio^{a,b}**INFN Sezione di Torino ^a, Università di Torino ^b, Torino, Italy, Università del Piemonte Orientale ^c, Novara, Italy**N. Amapane^{a,b}, R. Arcidiacono^{a,c,18}, S. Argiro^{a,b}, M. Arneodo^{a,c}, N. Bartosik^a, R. Bellan^{a,b}, C. Biino^a, N. Cartiglia^a, F. Cenna^{a,b}, M. Costa^{a,b}, R. Covarelli^{a,b}, A. Degano^{a,b}, N. Demaria^a, L. Finco^{a,b}, B. Kiani^{a,b}, C. Mariotti^a, S. Maselli^a, E. Migliore^{a,b}, V. Monaco^{a,b}, E. Monteil^{a,b},

M. Monteno^a, M.M. Obertino^{a,b}, L. Pacher^{a,b}, N. Pastrone^a, M. Pelliccioni^a, G.L. Pinna Angioni^{a,b}, F. Ravera^{a,b}, A. Romero^{a,b}, M. Ruspa^{a,c}, R. Sacchi^{a,b}, K. Shchelina^{a,b}, V. Sola^a, A. Solano^{a,b}, A. Staiano^a, P. Traczyk^{a,b}

INFN Sezione di Trieste ^a, Università di Trieste ^b, Trieste, Italy
S. Belforte^a, M. Casarsa^a, F. Cossutti^a, G. Della Ricca^{a,b}, A. Zanetti^a

Kyungpook National University, Daegu, Korea

D.H. Kim, G.N. Kim, M.S. Kim, S. Lee, S.W. Lee, Y.D. Oh, S. Sekmen, D.C. Son, Y.C. Yang

Chonbuk National University, Jeonju, Korea

A. Lee

Chonnam National University, Institute for Universe and Elementary Particles, Kwangju, Korea

H. Kim

Hanyang University, Seoul, Korea

J.A. Brochero Cifuentes, T.J. Kim

Korea University, Seoul, Korea

S. Cho, S. Choi, Y. Go, D. Gyun, S. Ha, B. Hong, Y. Jo, Y. Kim, K. Lee, K.S. Lee, S. Lee, J. Lim, S.K. Park, Y. Roh

Seoul National University, Seoul, Korea

J. Almond, J. Kim, H. Lee, S.B. Oh, B.C. Radburn-Smith, S.h. Seo, U.K. Yang, H.D. Yoo, G.B. Yu

University of Seoul, Seoul, Korea

M. Choi, H. Kim, J.H. Kim, J.S.H. Lee, I.C. Park, G. Ryu, M.S. Ryu

Sungkyunkwan University, Suwon, Korea

Y. Choi, J. Goh, C. Hwang, J. Lee, I. Yu

Vilnius University, Vilnius, Lithuania

V. Dudenas, A. Juodagalvis, J. Vaitkus

National Centre for Particle Physics, Universiti Malaya, Kuala Lumpur, Malaysia

I. Ahmed, Z.A. Ibrahim, M.A.B. Md Ali³⁵, F. Mohamad Idris³⁶, W.A.T. Wan Abdullah, M.N. Yusli, Z. Zolkapli

Centro de Investigacion y de Estudios Avanzados del IPN, Mexico City, Mexico

H. Castilla-Valdez, E. De La Cruz-Burelo, I. Heredia-De La Cruz³⁷, A. Hernandez-Almada, R. Lopez-Fernandez, R. Magaña Villalba, J. Mejia Guisao, A. Sanchez-Hernandez

Universidad Iberoamericana, Mexico City, Mexico

S. Carrillo Moreno, C. Oropeza Barrera, F. Vazquez Valencia

Benemerita Universidad Autonoma de Puebla, Puebla, Mexico

S. Carpintero, I. Pedraza, H.A. Salazar Ibarguen, C. Uribe Estrada

Universidad Autónoma de San Luis Potosí, San Luis Potosí, Mexico

A. Morelos Pineda

University of Auckland, Auckland, New Zealand

D. Kofcheck

University of Canterbury, Christchurch, New Zealand

P.H. Butler

National Centre for Physics, Quaid-I-Azam University, Islamabad, Pakistan

A. Ahmad, M. Ahmad, Q. Hassan, H.R. Hoorani, W.A. Khan, A. Saddique, M.A. Shah, M. Shoaib, M. Waqas

National Centre for Nuclear Research, Swierk, Poland

H. Bialkowska, M. Bluj, B. Boimska, T. Frueboes, M. Górski, M. Kazana, K. Nawrocki, K. Romanowska-Rybinska, M. Szleper, P. Zalewski

Institute of Experimental Physics, Faculty of Physics, University of Warsaw, Warsaw, Poland

K. Bunkowski, A. Byszuk³⁸, K. Doroba, A. Kalinowski, M. Konecki, J. Krolikowski, M. Misiura, M. Olszewski, M. Walczak

Laboratório de Instrumentação e Física Experimental de Partículas, Lisboa, Portugal

P. Bargassa, C. Beirão Da Cruz E Silva, B. Calpas, A. Di Francesco, P. Faccioli, P.G. Ferreira Parracho, M. Gallinaro, J. Hollar, N. Leonardo, L. Lloret Iglesias, M.V. Nemallapudi, J. Rodrigues Antunes, J. Seixas, O. Toldaiev, D. Vadruccio, J. Varela

Joint Institute for Nuclear Research, Dubna, Russia

S. Afanasiev, P. Bunin, M. Gavrilenco, I. Golutvin, I. Gorbunov, A. Kamenev, V. Karjavin, A. Lanev, A. Malakhov, V. Matveev^{39,40}, V. Palichik, V. Perelygin, S. Shmatov, S. Shulha, N. Skatchkov, V. Smirnov, N. Voytishin, A. Zarubin

Petersburg Nuclear Physics Institute, Gatchina (St. Petersburg), Russia

L. Chtchipounov, V. Golovtsov, Y. Ivanov, V. Kim⁴¹, E. Kuznetsova⁴², V. Murzin, V. Oreshkin, V. Sulimov, A. Vorobyev

Institute for Nuclear Research, Moscow, Russia

Yu. Andreev, A. Dermenev, S. Gninenko, N. Golubev, A. Karneyeu, M. Kirsanov, N. Krasnikov, A. Pashenkov, D. Tlisov, A. Toropin

Institute for Theoretical and Experimental Physics, Moscow, Russia

V. Epshteyn, V. Gavrilov, N. Lychkovskaya, V. Popov, I. Pozdnyakov, G. Safronov, A. Spiridonov, M. Toms, E. Vlasov, A. Zhokin

Moscow Institute of Physics and Technology, Moscow, Russia

T. Aushev, A. Bylinkin⁴⁰

National Research Nuclear University 'Moscow Engineering Physics Institute' (MEPhI), Moscow, Russia

R. Chistov⁴³, M. Danilov⁴³, E. Popova

P.N. Lebedev Physical Institute, Moscow, Russia

V. Andreev, M. Azarkin⁴⁰, I. Dremin⁴⁰, M. Kirakosyan, A. Leonidov⁴⁰, A. Terkulov

Skobeltsyn Institute of Nuclear Physics, Lomonosov Moscow State University, Moscow, Russia

A. Baskakov, A. Belyaev, E. Boos, A. Gribushin, L. Khein, V. Klyukhin, O. Kodolova, I. Loktin, O. Lukina, I. Miagkov, S. Obraztsov, S. Petrushanko, V. Savrin, A. Snigirev, P. Volkov

Novosibirsk State University (NSU), Novosibirsk, Russia

V. Blinov⁴⁴, Y. Skovpen⁴⁴, D. Shtol⁴⁴

State Research Center of Russian Federation, Institute for High Energy Physics, Protvino, Russia

I. Azhgirey, I. Bayshev, S. Bitioukov, D. Elumakhov, V. Kachanov, A. Kalinin, D. Konstantinov, V. Krychkine, V. Petrov, R. Ryutin, A. Sobol, S. Troshin, N. Tyurin, A. Uzunian, A. Volkov

University of Belgrade, Faculty of Physics and Vinca Institute of Nuclear Sciences, Belgrade, Serbia

P. Adzic⁴⁵, P. Cirkovic, D. Devetak, M. Dordevic, J. Milosevic, V. Rekovic

Centro de Investigaciones Energéticas Medioambientales y Tecnológicas (CIEMAT), Madrid, Spain

J. Alcaraz Maestre, M. Barrio Luna, E. Calvo, M. Cerrada, M. Chamizo Llatas, N. Colino, B. De La Cruz, A. Delgado Peris, A. Escalante Del Valle, C. Fernandez Bedoya, J.P. Fernández Ramos, J. Flix, M.C. Fouz, P. Garcia-Abia, O. Gonzalez Lopez, S. Goy Lopez, J.M. Hernandez, M.I. Josa, E. Navarro De Martino, A. Pérez-Calero Yzquierdo, J. Puerta Pelayo, A. Quintario Olmeda, I. Redondo, L. Romero, M.S. Soares

Universidad Autónoma de Madrid, Madrid, Spain

J.F. de Trocóniz, M. Missiroli, D. Moran

Universidad de Oviedo, Oviedo, Spain

J. Cuevas, J. Fernandez Menendez, I. Gonzalez Caballero, J.R. González Fernández, E. Palencia Cortezon, S. Sanchez Cruz, I. Suárez Andrés, P. Vischia, J.M. Vizan Garcia

Instituto de Física de Cantabria (IFCA), CSIC-Universidad de Cantabria, Santander, Spain

I.J. Cabrillo, A. Calderon, E. Curras, M. Fernandez, J. Garcia-Ferrero, G. Gomez, A. Lopez Virto, J. Marco, C. Martinez Rivero, F. Matorras, J. Piedra Gomez, T. Rodrigo, A. Ruiz-Jimeno, L. Scodellaro, N. Trevisani, I. Vila, R. Vilar Cortabitarte

CERN, European Organization for Nuclear Research, Geneva, Switzerland

D. Abbaneo, E. Auffray, G. Auzinger, P. Baillon, A.H. Ball, D. Barney, P. Bloch, A. Bocci, C. Botta, T. Camporesi, R. Castello, M. Cepeda, G. Cerminara, Y. Chen, D. d'Enterria, A. Dabrowski, V. Daponte, A. David, M. De Gruttola, A. De Roeck, E. Di Marco⁴⁶, M. Dobson, B. Dorney, T. du Pree, D. Duggan, M. Dünser, N. Dupont, A. Elliott-Peisert, P. Everaerts, S. Fartoukh, G. Franzoni, J. Fulcher, W. Funk, D. Gigi, K. Gill, M. Girone, F. Glege, D. Gulhan, S. Gundacker, M. Guthoff, P. Harris, J. Hegeman, V. Innocente, P. Janot, J. Kieseler, H. Kirschenmann, V. Knünz, A. Kornmayer¹⁸, M.J. Kortelainen, K. Kousouris, M. Krammer¹, C. Lange, P. Lecoq, C. Lourenço, M.T. Lucchini, L. Malgeri, M. Mannelli, A. Martelli, F. Meijers, J.A. Merlin, S. Mersi, E. Meschi, P. Milenovic⁴⁷, F. Moortgat, S. Morovic, M. Mulders, H. Neugebauer, S. Orfanelli, L. Orsini, L. Pape, E. Perez, M. Peruzzi, A. Petrilli, G. Petrucciani, A. Pfeiffer, M. Pierini, A. Racz, T. Reis, G. Rolandi⁴⁸, M. Rovere, H. Sakulin, J.B. Sauvan, C. Schäfer, C. Schwick, M. Seidel, A. Sharma, P. Silva, P. Sphicas⁴⁹, J. Steggemann, M. Stoye, Y. Takahashi, M. Tosi, D. Treille, A. Triossi, A. Tsirou, V. Veckalns⁵⁰, G.I. Veres²³, M. Verweij, N. Wardle, H.K. Wöhri, A. Zagozdzinska³⁸, W.D. Zeuner

Paul Scherrer Institut, Villigen, Switzerland

W. Bertl, K. Deiters, W. Erdmann, R. Horisberger, Q. Ingram, H.C. Kaestli, D. Kotlinski, U. Langenegger, T. Rohe, S.A. Wiederkehr

Institute for Particle Physics, ETH Zurich, Zurich, Switzerland

F. Bachmair, L. Bäni, L. Bianchini, B. Casal, G. Dissertori, M. Dittmar, M. Donegà, C. Grab, C. Heidegger, D. Hits, J. Hoss, G. Kasieczka, W. Lustermann, B. Mangano, M. Marionneau, P. Martinez Ruiz del Arbol, M. Masciovecchio, M.T. Meinhard, D. Meister, F. Michelini, P. Musella, F. Nessi-Tedaldi, F. Pandolfi, J. Pata, F. Pauss, G. Perrin, L. Perrozzi, M. Quittnat, M. Rossini, M. Schönenberger, A. Starodumov⁵¹, V.R. Tavolaro, K. Theofilatos, R. Wallny

Universität Zürich, Zurich, Switzerland

T.K. Arrestad, C. Amsler⁵², L. Caminada, M.F. Canelli, A. De Cosa, C. Galloni, A. Hinzmann,

T. Hreus, B. Kilminster, J. Ngadiuba, D. Pinna, G. Rauco, P. Robmann, D. Salerno, C. Seitz, Y. Yang, A. Zucchetta

National Central University, Chung-Li, Taiwan

V. Candelise, T.H. Doan, Sh. Jain, R. Khurana, M. Konyushikhin, C.M. Kuo, W. Lin, A. Pozdnyakov, S.S. Yu

National Taiwan University (NTU), Taipei, Taiwan

Arun Kumar, P. Chang, Y.H. Chang, Y. Chao, K.F. Chen, P.H. Chen, F. Fiori, W.-S. Hou, Y. Hsiung, Y.F. Liu, R.-S. Lu, M. Miñano Moya, E. Paganis, A. Psallidas, J.f. Tsai

Chulalongkorn University, Faculty of Science, Department of Physics, Bangkok, Thailand

B. Asavapibhop, G. Singh, N. Srimanobhas, N. Suwonjandee

Cukurova University, Physics Department, Science and Art Faculty, Adana, Turkey

A. Adiguzel, M.N. Bakirci⁵³, S. Cerci⁵⁴, S. Damarseckin, Z.S. Demiroglu, C. Dozen, I. Dumanoglu, S. Giris, G. Gokbulut, Y. Guler, I. Hos⁵⁵, E.E. Kangal⁵⁶, O. Kara, A. Kayis Topaksu, U. Kiminsu, M. Oglakci, G. Onengut⁵⁷, K. Ozdemir⁵⁸, B. Tali⁵⁴, S. Turkcapar, I.S. Zorbakir, C. Zorbilmez

Middle East Technical University, Physics Department, Ankara, Turkey

B. Bilin, S. Bilmis, B. Isildak⁵⁹, G. Karapinar⁶⁰, M. Yalvac, M. Zeyrek

Bogazici University, Istanbul, Turkey

E. Gülmez, M. Kaya⁶¹, O. Kaya⁶², E.A. Yetkin⁶³, T. Yetkin⁶⁴

Istanbul Technical University, Istanbul, Turkey

A. Cakir, K. Cankocak, S. Sen⁶⁵

Institute for Scintillation Materials of National Academy of Science of Ukraine, Kharkov, Ukraine

B. Grynyov

National Scientific Center, Kharkov Institute of Physics and Technology, Kharkov, Ukraine

L. Levchuk, P. Sorokin

University of Bristol, Bristol, United Kingdom

R. Aggleton, F. Ball, L. Beck, J.J. Brooke, D. Burns, E. Clement, D. Cussans, H. Flacher, J. Goldstein, M. Grimes, G.P. Heath, H.F. Heath, J. Jacob, L. Kreczko, C. Lucas, D.M. Newbold⁶⁶, S. Paramesvaran, A. Poll, T. Sakuma, S. Seif El Nasr-storey, D. Smith, V.J. Smith

Rutherford Appleton Laboratory, Didcot, United Kingdom

K.W. Bell, A. Belyaev⁶⁷, C. Brew, R.M. Brown, L. Calligaris, D. Cieri, D.J.A. Cockerill, J.A. Coughlan, K. Harder, S. Harper, E. Olaiya, D. Petyt, C.H. Shepherd-Themistocleous, A. Thea, I.R. Tomalin, T. Williams

Imperial College, London, United Kingdom

M. Baber, R. Bainbridge, O. Buchmuller, A. Bundock, D. Burton, S. Casasso, M. Citron, D. Colling, L. Corpe, P. Dauncey, G. Davies, A. De Wit, M. Della Negra, R. Di Maria, P. Dunne, A. Elwood, D. Fulyan, Y. Haddad, G. Hall, G. Iles, T. James, R. Lane, C. Laner, R. Lucas⁶⁶, L. Lyons, A.-M. Magnan, S. Malik, L. Mastrolorenzo, J. Nash, A. Nikitenko⁵¹, J. Pela, B. Penning, M. Pesaresi, D.M. Raymond, A. Richards, A. Rose, E. Scott, C. Seez, S. Summers, A. Tapper, K. Uchida, M. Vazquez Acosta⁶⁸, T. Virdee¹⁸, J. Wright, S.C. Zenz

Brunel University, Uxbridge, United Kingdom

J.E. Cole, P.R. Hobson, A. Khan, P. Kyberd, I.D. Reid, P. Symonds, L. Teodorescu, M. Turner

Baylor University, Waco, USA

A. Borzou, K. Call, J. Dittmann, K. Hatakeyama, H. Liu, N. Pastika

Catholic University of America, Washington, USA

R. Bartek, A. Dominguez

The University of Alabama, Tuscaloosa, USA

A. Buccilli, S.I. Cooper, C. Henderson, P. Rumerio, C. West

Boston University, Boston, USA

D. Arcaro, A. Avetisyan, T. Bose, D. Gastler, D. Rankin, C. Richardson, J. Rohlf, L. Sulak, D. Zou

Brown University, Providence, USA

G. Benelli, D. Cutts, A. Garabedian, J. Hakala, U. Heintz, J.M. Hogan, O. Jesus, K.H.M. Kwok, E. Laird, G. Landsberg, Z. Mao, M. Narain, S. Piperov, S. Sagir, E. Spencer, R. Syarif

University of California, Davis, Davis, USA

R. Breedon, D. Burns, M. Calderon De La Barca Sanchez, S. Chauhan, M. Chertok, J. Conway, R. Conway, P.T. Cox, R. Erbacher, C. Flores, G. Funk, M. Gardner, W. Ko, R. Lander, C. Mclean, M. Mulhearn, D. Pellett, J. Pilot, S. Shalhout, M. Shi, J. Smith, M. Squires, D. Stolp, K. Tos, M. Tripathi

University of California, Los Angeles, USA

M. Bachtis, C. Bravo, R. Cousins, A. Dasgupta, A. Florent, J. Hauser, M. Ignatenko, N. Mccoll, D. Saltzberg, C. Schnaible, V. Valuev, M. Weber

University of California, Riverside, Riverside, USA

E. Bouvier, K. Burt, R. Clare, J. Ellison, J.W. Gary, S.M.A. Ghiasi Shirazi, G. Hanson, J. Heilman, P. Jandir, E. Kennedy, F. Lacroix, O.R. Long, M. Olmedo Negrete, M.I. Paneva, A. Shrinivas, W. Si, H. Wei, S. Wimpenny, B. R. Yates

University of California, San Diego, La Jolla, USA

J.G. Branson, G.B. Cerati, S. Cittolin, M. Derdzinski, R. Gerosa, A. Holzner, D. Klein, V. Krutelyov, J. Letts, I. Macneill, D. Olivito, S. Padhi, M. Pieri, M. Sani, V. Sharma, S. Simon, M. Tadel, A. Vartak, S. Wasserbaech⁶⁹, C. Welke, J. Wood, F. Würthwein, A. Yagil, G. Zevi Della Porta

University of California, Santa Barbara - Department of Physics, Santa Barbara, USA

N. Amin, R. Bhandari, J. Bradmiller-Feld, C. Campagnari, A. Dishaw, V. Dutta, M. Franco Sevilla, C. George, F. Golf, L. Gouskos, J. Gran, R. Heller, J. Incandela, S.D. Mullin, A. Ovcharova, H. Qu, J. Richman, D. Stuart, I. Suarez, J. Yoo

California Institute of Technology, Pasadena, USA

D. Anderson, J. Bendavid, A. Bornheim, J. Bunn, J. Duarte, J.M. Lawhorn, A. Mott, H.B. Newman, C. Pena, M. Spiropulu, J.R. Vlimant, S. Xie, R.Y. Zhu

Carnegie Mellon University, Pittsburgh, USA

M.B. Andrews, T. Ferguson, M. Paulini, J. Russ, M. Sun, H. Vogel, I. Vorobiev, M. Weinberg

University of Colorado Boulder, Boulder, USA

J.P. Cumalat, W.T. Ford, F. Jensen, A. Johnson, M. Krohn, S. Leontsinis, T. Mulholland, K. Stenson, S.R. Wagner

Cornell University, Ithaca, USA

J. Alexander, J. Chaves, J. Chu, S. Dittmer, K. Mcdermott, N. Mirman, G. Nicolas Kaufman,

J.R. Patterson, A. Rinkevicius, A. Ryd, L. Skinnari, L. Soffi, S.M. Tan, Z. Tao, J. Thom, J. Tucker, P. Wittich, M. Zientek

Fairfield University, Fairfield, USA

D. Winn

Fermi National Accelerator Laboratory, Batavia, USA

S. Abdullin, M. Albrow, G. Apollinari, A. Apresyan, S. Banerjee, L.A.T. Bauerick, A. Beretvas, J. Berryhill, P.C. Bhat, G. Bolla, K. Burkett, J.N. Butler, H.W.K. Cheung, F. Chlebana, S. Cihangir[†], M. Cremonesi, V.D. Elvira, I. Fisk, J. Freeman, E. Gottschalk, L. Gray, D. Green, S. Grünendahl, O. Gutsche, D. Hare, R.M. Harris, S. Hasegawa, J. Hirschauer, Z. Hu, B. Jayatilaka, S. Jindariani, M. Johnson, U. Joshi, B. Klima, B. Kreis, S. Lammel, J. Linacre, D. Lincoln, R. Lipton, M. Liu, T. Liu, R. Lopes De Sá, J. Lykken, K. Maeshima, N. Magini, J.M. Marraffino, S. Maruyama, D. Mason, P. McBride, P. Merkel, S. Mrenna, S. Nahn, V. O'Dell, K. Pedro, O. Prokofyev, G. Rakness, L. Ristori, E. Sexton-Kennedy, A. Soha, W.J. Spalding, L. Spiegel, S. Stoynev, J. Strait, N. Strobbe, L. Taylor, S. Tkaczyk, N.V. Tran, L. Uplegger, E.W. Vaandering, C. Vernieri, M. Verzocchi, R. Vidal, M. Wang, H.A. Weber, A. Whitbeck, Y. Wu

University of Florida, Gainesville, USA

D. Acosta, P. Avery, P. Bortignon, D. Bourilkov, A. Brinkerhoff, A. Carnes, M. Carver, D. Curry, S. Das, R.D. Field, I.K. Furic, J. Konigsberg, A. Korytov, J.F. Low, P. Ma, K. Matchev, H. Mei, G. Mitselmakher, D. Rank, L. Shchutska, D. Sperka, L. Thomas, J. Wang, S. Wang, J. Yelton

Florida International University, Miami, USA

S. Linn, P. Markowitz, G. Martinez, J.L. Rodriguez

Florida State University, Tallahassee, USA

A. Ackert, T. Adams, A. Askew, S. Bein, S. Hagopian, V. Hagopian, K.F. Johnson, T. Kolberg, H. Prosper, A. Santra, R. Yohay

Florida Institute of Technology, Melbourne, USA

M.M. Baarmand, V. Bhopatkar, S. Colafranceschi, M. Hohlmann, D. Noonan, T. Roy, F. Yumiceva

University of Illinois at Chicago (UIC), Chicago, USA

M.R. Adams, L. Apanasevich, D. Berry, R.R. Betts, I. Bucinskaite, R. Cavanaugh, O. Evdokimov, L. Gauthier, C.E. Gerber, D.J. Hofman, K. Jung, I.D. Sandoval Gonzalez, N. Varelas, H. Wang, Z. Wu, M. Zakaria, J. Zhang

The University of Iowa, Iowa City, USA

B. Bilki⁷⁰, W. Clarida, K. Dilsiz, S. Durgut, R.P. Gundrajula, M. Haytmyradov, V. Khristenko, J.-P. Merlo, H. Mermerkaya⁷¹, A. Mestvirishvili, A. Moeller, J. Nachtman, H. Ogul, Y. Onel, F. Ozok⁷², A. Penzo, C. Snyder, E. Tiras, J. Wetzel, K. Yi

Johns Hopkins University, Baltimore, USA

B. Blumenfeld, A. Cocoros, N. Eminizer, D. Fehling, L. Feng, A.V. Gritsan, P. Maksimovic, J. Roskes, U. Sarica, M. Swartz, M. Xiao, C. You

The University of Kansas, Lawrence, USA

A. Al-bataineh, P. Baringer, A. Bean, S. Boren, J. Bowen, J. Castle, L. Forthomme, R.P. Kenny III, S. Khalil, A. Kropivnitskaya, D. Majumder, W. Mcbrayer, M. Murray, S. Sanders, R. Stringer, J.D. Tapia Takaki, Q. Wang

Kansas State University, Manhattan, USA

A. Ivanov, K. Kaadze, Y. Maravin, A. Mohammadi, L.K. Saini, N. Skhirtladze, S. Toda

Lawrence Livermore National Laboratory, Livermore, USA

F. Rebassoo, D. Wright

University of Maryland, College Park, USA

C. Anelli, A. Baden, O. Baron, A. Belloni, B. Calvert, S.C. Eno, C. Ferraioli, J.A. Gomez, N.J. Hadley, S. Jabeen, G.Y. Jeng, R.G. Kellogg, J. Kunkle, A.C. Mignerey, F. Ricci-Tam, Y.H. Shin, A. Skuja, M.B. Tonjes, S.C. Tonwar

Massachusetts Institute of Technology, Cambridge, USA

D. Abercrombie, B. Allen, A. Apyan, V. Azzolini, R. Barbieri, A. Baty, R. Bi, K. Bierwagen, S. Brandt, W. Busza, I.A. Cali, M. D'Alfonso, Z. Demiragli, G. Gomez Ceballos, M. Goncharov, D. Hsu, Y. Iiyama, G.M. Innocenti, M. Klute, D. Kovalevskyi, K. Krafczak, Y.S. Lai, Y.-J. Lee, A. Levin, P.D. Luckey, B. Maier, A.C. Marini, C. McGinn, C. Mironov, S. Narayanan, X. Niu, C. Paus, C. Roland, G. Roland, J. Salfeld-Nebgen, G.S.F. Stephans, K. Tatar, D. Velicanu, J. Wang, T.W. Wang, B. Wyslouch

University of Minnesota, Minneapolis, USA

A.C. Benvenuti, R.M. Chatterjee, A. Evans, P. Hansen, S. Kalafut, S.C. Kao, Y. Kubota, Z. Lesko, J. Mans, S. Nourbakhsh, N. Ruckstuhl, R. Rusack, N. Tambe, J. Turkewitz

University of Mississippi, Oxford, USA

J.G. Acosta, S. Oliveros

University of Nebraska-Lincoln, Lincoln, USA

E. Avdeeva, K. Bloom, D.R. Claes, C. Fangmeier, R. Gonzalez Suarez, R. Kamalieddin, I. Kravchenko, A. Malta Rodrigues, J. Monroy, J.E. Siado, G.R. Snow, B. Stieger

State University of New York at Buffalo, Buffalo, USA

M. Alyari, J. Dolen, A. Godshalk, C. Harrington, I. Iashvili, J. Kaisen, D. Nguyen, A. Parker, S. Rappoccio, B. Roozbahani

Northeastern University, Boston, USA

G. Alverson, E. Barberis, A. Hortiangtham, A. Massironi, D.M. Morse, D. Nash, T. Orimoto, R. Teixeira De Lima, D. Trocino, R.-J. Wang, D. Wood

Northwestern University, Evanston, USA

S. Bhattacharya, O. Charaf, K.A. Hahn, A. Kumar, N. Mucia, N. Odell, B. Pollack, M.H. Schmitt, K. Sung, M. Trovato, M. Velasco

University of Notre Dame, Notre Dame, USA

N. Dev, M. Hildreth, K. Hurtado Anampa, C. Jessop, D.J. Karmgard, N. Kellams, K. Lannon, N. Marinelli, F. Meng, C. Mueller, Y. Musienko³⁹, M. Planer, A. Reinsvold, R. Ruchti, N. Rupprecht, G. Smith, S. Taroni, M. Wayne, M. Wolf, A. Woodard

The Ohio State University, Columbus, USA

J. Alimena, L. Antonelli, B. Bylsma, L.S. Durkin, S. Flowers, B. Francis, A. Hart, C. Hill, R. Hughes, W. Ji, B. Liu, W. Luo, D. Puigh, B.L. Winer, H.W. Wulsin

Princeton University, Princeton, USA

S. Cooperstein, O. Driga, P. Elmer, J. Hardenbrook, P. Hebda, D. Lange, J. Luo, D. Marlow, T. Medvedeva, K. Mei, I. Ojalvo, J. Olsen, C. Palmer, P. Piroué, D. Stickland, A. Svyatkovskiy, C. Tully

University of Puerto Rico, Mayaguez, USA

S. Malik

Purdue University, West Lafayette, USA

A. Barker, V.E. Barnes, S. Folgueras, L. Gutay, M.K. Jha, M. Jones, A.W. Jung, A. Khatiwada, D.H. Miller, N. Neumeister, J.F. Schulte, X. Shi, J. Sun, F. Wang, W. Xie

Purdue University Northwest, Hammond, USA

N. Parashar, J. Stupak

Rice University, Houston, USA

A. Adair, B. Akgun, Z. Chen, K.M. Ecklund, F.J.M. Geurts, M. Guilbaud, W. Li, B. Michlin, M. Northup, B.P. Padley, J. Roberts, J. Rorie, Z. Tu, J. Zabel

University of Rochester, Rochester, USA

B. Betchart, A. Bodek, P. de Barbaro, R. Demina, Y.t. Duh, T. Ferbel, M. Galanti, A. Garcia-Bellido, J. Han, O. Hindrichs, A. Khukhunaishvili, K.H. Lo, P. Tan, M. Verzetti

Rutgers, The State University of New Jersey, Piscataway, USA

A. Agapitos, J.P. Chou, Y. Gershtein, T.A. Gómez Espinosa, E. Halkiadakis, M. Heindl, E. Hughes, S. Kaplan, R. Kunnnawalkam Elayavalli, S. Kyriacou, A. Lath, K. Nash, M. Osherson, H. Saka, S. Salur, S. Schnetzer, D. Sheffield, S. Somalwar, R. Stone, S. Thomas, P. Thomassen, M. Walker

University of Tennessee, Knoxville, USA

A.G. Delannoy, M. Foerster, J. Heideman, G. Riley, K. Rose, S. Spanier, K. Thapa

Texas A&M University, College Station, USA

O. Bouhali⁷³, A. Celik, M. Dalchenko, M. De Mattia, A. Delgado, S. Dildick, R. Eusebi, J. Gilmore, T. Huang, E. Juska, T. Kamon⁷⁴, R. Mueller, Y. Pakhotin, R. Patel, A. Perloff, L. Perniè, D. Rathjens, A. Safonov, A. Tatarinov, K.A. Ulmer

Texas Tech University, Lubbock, USA

N. Akchurin, J. Damgov, F. De Guio, C. Dragoiu, P.R. Dudero, J. Faulkner, E. Gurpinar, S. Kunori, K. Lamichhane, S.W. Lee, T. Libeiro, T. Peltola, S. Undleeb, I. Volobouev, Z. Wang

Vanderbilt University, Nashville, USA

S. Greene, A. Gurrola, R. Janjam, W. Johns, C. Maguire, A. Melo, H. Ni, P. Sheldon, S. Tuo, J. Velkovska, Q. Xu

University of Virginia, Charlottesville, USA

M.W. Arenton, P. Barria, B. Cox, J. Goodell, R. Hirosky, A. Ledovskoy, H. Li, C. Neu, T. Sinthuprasith, X. Sun, Y. Wang, E. Wolfe, F. Xia

Wayne State University, Detroit, USA

C. Clarke, R. Harr, P.E. Karchin, J. Sturdy

University of Wisconsin - Madison, Madison, WI, USA

D.A. Belknap, J. Buchanan, C. Caillol, S. Dasu, L. Dodd, S. Duric, B. Gomber, M. Grothe, M. Herndon, A. Hervé, P. Klabbers, A. Lanaro, A. Levine, K. Long, R. Loveless, T. Perry, G.A. Pierro, G. Polese, T. Ruggles, A. Savin, N. Smith, W.H. Smith, D. Taylor, N. Woods

†: Deceased

1: Also at Vienna University of Technology, Vienna, Austria

2: Also at State Key Laboratory of Nuclear Physics and Technology, Peking University, Beijing, China

3: Also at Institut Pluridisciplinaire Hubert Curien (IPHC), Université de Strasbourg, CNRS/IN2P3, Strasbourg, France

-
- 4: Also at Universidade Estadual de Campinas, Campinas, Brazil
 - 5: Also at Universidade Federal de Pelotas, Pelotas, Brazil
 - 6: Also at Université Libre de Bruxelles, Bruxelles, Belgium
 - 7: Also at Deutsches Elektronen-Synchrotron, Hamburg, Germany
 - 8: Also at Universidad de Antioquia, Medellin, Colombia
 - 9: Also at Joint Institute for Nuclear Research, Dubna, Russia
 - 10: Also at Helwan University, Cairo, Egypt
 - 11: Now at Zewail City of Science and Technology, Zewail, Egypt
 - 12: Now at Fayoum University, El-Fayoum, Egypt
 - 13: Also at British University in Egypt, Cairo, Egypt
 - 14: Now at Ain Shams University, Cairo, Egypt
 - 15: Also at Université de Haute Alsace, Mulhouse, France
 - 16: Also at Skobeltsyn Institute of Nuclear Physics, Lomonosov Moscow State University, Moscow, Russia
 - 17: Also at Tbilisi State University, Tbilisi, Georgia
 - 18: Also at CERN, European Organization for Nuclear Research, Geneva, Switzerland
 - 19: Also at RWTH Aachen University, III. Physikalisches Institut A, Aachen, Germany
 - 20: Also at University of Hamburg, Hamburg, Germany
 - 21: Also at Brandenburg University of Technology, Cottbus, Germany
 - 22: Also at Institute of Nuclear Research ATOMKI, Debrecen, Hungary
 - 23: Also at MTA-ELTE Lendület CMS Particle and Nuclear Physics Group, Eötvös Loránd University, Budapest, Hungary
 - 24: Also at Institute of Physics, University of Debrecen, Debrecen, Hungary
 - 25: Also at Indian Institute of Technology Bhubaneswar, Bhubaneswar, India
 - 26: Also at University of Visva-Bharati, Santiniketan, India
 - 27: Also at Indian Institute of Science Education and Research, Bhopal, India
 - 28: Also at Institute of Physics, Bhubaneswar, India
 - 29: Also at University of Ruhuna, Matara, Sri Lanka
 - 30: Also at Isfahan University of Technology, Isfahan, Iran
 - 31: Also at Yazd University, Yazd, Iran
 - 32: Also at Plasma Physics Research Center, Science and Research Branch, Islamic Azad University, Tehran, Iran
 - 33: Also at Università degli Studi di Siena, Siena, Italy
 - 34: Also at Purdue University, West Lafayette, USA
 - 35: Also at International Islamic University of Malaysia, Kuala Lumpur, Malaysia
 - 36: Also at Malaysian Nuclear Agency, MOSTI, Kajang, Malaysia
 - 37: Also at Consejo Nacional de Ciencia y Tecnología, Mexico city, Mexico
 - 38: Also at Warsaw University of Technology, Institute of Electronic Systems, Warsaw, Poland
 - 39: Also at Institute for Nuclear Research, Moscow, Russia
 - 40: Now at National Research Nuclear University 'Moscow Engineering Physics Institute' (MEPhI), Moscow, Russia
 - 41: Also at St. Petersburg State Polytechnical University, St. Petersburg, Russia
 - 42: Also at University of Florida, Gainesville, USA
 - 43: Also at P.N. Lebedev Physical Institute, Moscow, Russia
 - 44: Also at Budker Institute of Nuclear Physics, Novosibirsk, Russia
 - 45: Also at Faculty of Physics, University of Belgrade, Belgrade, Serbia
 - 46: Also at INFN Sezione di Roma; Sapienza Università di Roma, Rome, Italy
 - 47: Also at University of Belgrade, Faculty of Physics and Vinca Institute of Nuclear Sciences, Belgrade, Serbia

- 48: Also at Scuola Normale e Sezione dell'INFN, Pisa, Italy
- 49: Also at National and Kapodistrian University of Athens, Athens, Greece
- 50: Also at Riga Technical University, Riga, Latvia
- 51: Also at Institute for Theoretical and Experimental Physics, Moscow, Russia
- 52: Also at Albert Einstein Center for Fundamental Physics, Bern, Switzerland
- 53: Also at Gaziosmanpasa University, Tokat, Turkey
- 54: Also at Adiyaman University, Adiyaman, Turkey
- 55: Also at Istanbul Aydin University, Istanbul, Turkey
- 56: Also at Mersin University, Mersin, Turkey
- 57: Also at Cag University, Mersin, Turkey
- 58: Also at Piri Reis University, Istanbul, Turkey
- 59: Also at Ozyegin University, Istanbul, Turkey
- 60: Also at Izmir Institute of Technology, Izmir, Turkey
- 61: Also at Marmara University, Istanbul, Turkey
- 62: Also at Kafkas University, Kars, Turkey
- 63: Also at Istanbul Bilgi University, Istanbul, Turkey
- 64: Also at Yildiz Technical University, Istanbul, Turkey
- 65: Also at Hacettepe University, Ankara, Turkey
- 66: Also at Rutherford Appleton Laboratory, Didcot, United Kingdom
- 67: Also at School of Physics and Astronomy, University of Southampton, Southampton, United Kingdom
- 68: Also at Instituto de Astrofísica de Canarias, La Laguna, Spain
- 69: Also at Utah Valley University, Orem, USA
- 70: Also at Argonne National Laboratory, Argonne, USA
- 71: Also at Erzincan University, Erzincan, Turkey
- 72: Also at Mimar Sinan University, Istanbul, Istanbul, Turkey
- 73: Also at Texas A&M University at Qatar, Doha, Qatar
- 74: Also at Kyungpook National University, Daegu, Korea